PERGAMON

International Journal of Solids and Structures 39 (2002) 2235–2255

INTERNATIONAL JOURNAL OF SOLIDS and STRUCTURES

www.elsevier.com/locate/ijsolstr

Three-dimensional Green's functions in anisotropic trimaterials

B. Yang, E. Pan *

Structures Technology Inc., 543 Keisler Drive Suite 204, Cary, NC 27511, USA

Received 8 May 2001; received in revised form 4 December 2001

Abstract

Three-dimensional elastostatic Green's functions in anisotropic trimaterials are derived, *for the first time*, by applying the generalized Stroh's formalism and Fourier transforms. The Green's functions are expressed as a series summation with the first term corresponding to the full-space solution and other terms to the image solutions due to the interfaces. The most remarkable feature of the present solution is that the image solutions can be expressed by a simple line integral over a finite interval $[0, 2\pi]$. By partitioning the trimaterial Green's function into a full-space solution and a complementary part, the line integral involves only regular functions if the singularity is within one of the three materials, being treated analytically owning to the explicit expression of the full-space solution. When the singularity is on the interface, which occurs if the field and source points are both on the same interface, the involved singularity is handled with the interfacial Green's functions.

A numerical example is presented for a trimaterial system made of two anisotropic half spaces bonded perfectly by an isotropic adhesive layer, showing clearly the effect of material layering on the Green's displacements and stresses. Furthermore, by comparing the present Green's solution to the direct (two-dimensional) 2D integral expression which is also derived in this paper, it is shown that, the computational time for the calculation of the Green's function can be substantially reduced using the present solution, instead of the direct 2D integral method.

Keywords: Green's function; Stroh formalism; Anisotropic elasticity; Expansion solution; 3D trimaterial; Boundary integral equation method; Quantum-dot semiconductor devices

1. Introduction

Trimaterials are constructed by sandwiching a plate of uniform thickness with two opposite half-space media. The interfacial condition may be of perfect or imperfect bond. This structure is of particular interest in broad areas of engineering and physics, such as structural composite laminates (see, for example, Pagano (1978a, 1978b); Schoeppner and Pagano (1998) and Jones (1999)), and thin film and coating on substrates (see, for example, Hu (1991); Suo and Hutchinson (1989); Hutchinson and Suo (1991); Freund (1994); Gao

* Corresponding author. Tel.: +1-919-816-0434; fax: +1-919-816-0438.
E-mail address: ernian_pan@yahoo.com (E. Pan).

0020-7683/02/$ - see front matter
PII: S0020-7683(02)00088-4

and Nix (1999); Liu et al. (2000); Schweitz et al. (2000); Suhir (2000, 2001); Hsueh (2000) and Jenichen et al. (2001)). A fundamental solution, or a Green's function, in such a complicated structure is of great value since it can be directly implemented into a corresponding boundary integral equation formulation for a numerical study (see, i.e., Pan et al. (2001)). Furthermore, Green's function solution in trimaterials can be directly applied to the study of quantum-dot growth in modern semiconductor devices (Pearson and Faux, 2000; Pan and Yang, 2001). While the Green's functions for layered media of isotropic elasticity and two-dimensional (2D) anisotropic elasticity were extensively investigated previously (Mindlin, 1936; Chou, 1966; Fares and Li, 1988; Yu and Sanday, 1993; Pan, 1997; Shou and Napier, 1999; Shou, 2000), the Green's functions in the corresponding 3D anisotropic elasticity appears to be very limited (Barnett and Lothe, 1975; Ting, 1996; Wu, 1998; Pan and Yuan, 2000; Pan and Yang, submitted for publication). The earliest study in this area is, perhaps, by Barnett and Lothe (1975) where they derived the physical-domain surface Green's functions in a 3D half-space using the generalized Stroh formalism. Also applying the generalized Stroh formalism, Ting (1996) derived the 3D Green's function for anisotropic bimaterials in the transformed domain. Pan and Yuan (2000) further studied the features of the transformed bimaterial Green's function and analytically carried out the integral of the inverse transform in infinite radial direction in the polar coordinates. By doing so, the physical-domain Green's function for anisotropic bimaterials is obtained as a line integral over the interval $[0, \pi]$, reducing significantly the computational time in the evaluation of the Green's functions. More recently, Pan and Yang (submitted for publication) derived the interfacial Green's functions of anisotropic bimaterials where both the source and field points are on the interface plane. In this case, a special care is needed to handle the line integral due to the appearance of singularities up to the third order, one order higher than the common hypersingularity (Pan and Yang, submitted for publication).

The present work is to derive the 3D Green's functions for anisotropic trimaterials using the generalized Stroh's formalism (Barnett and Lothe, 1975; Ting, 1996; Pan and Yuan, 2000), 2D Fourier transform, and Mindlin's superposition method (Mindlin, 1936; Pan and Yuan, 2000). In the formalism, the Green's functions are first solved in the 2D Fourier transformed domain. Then, the Green's functions in the physical domain are obtained by the Fourier inverse transform. In order to handle the 2D Fourier integral, an expansion approach of truncated series is proposed. With this approach, each term in the truncated series can be successfully expressed as a line integral over the interval $[0, 2\pi]$. Consequently, the proposed expansion solution can substantially reduce the computational burden involved in the calculation of the 3D trimaterial Green's functions. A numerical example presented in the paper, using an adaptive quadrature scheme, shows that within an error of 5% on the calculation of the trimaterial Green's function, the expansion solution requires less than 10% of the computational time required by the direct 2D integral. Furthermore, we remark that the mathematically constructed expansion solution turns out to be similar to a physics-motivated solution by imaging the source across an interface between dissimilar media. The image method, as is well known, has been applied to solve many mechanical and physical problems (Fares and Li, 1988; Yu and Sanday, 1993; Shou and Napier, 1999; Shou, 2000). A similar approach, namely, eigenexpansion, was also proposed recently to solve certain 2D problems involving orthotropic and anisotropic strips (Matemilola and Stronge, 1995; Chiu and Wu, 1998).

This paper is organized as follows: In Section 2, a boundary-value problem of the anisotropic elastostatic trimaterial subjected to a point force is formulated. The three media are assumed to be bonded perfectly along the interfaces. In Section 3, the general solution in a homogeneous region by the generalized Stroh's formalism is summarized. In Section 4, the trimaterial Green's functions in the physical domain are constructed using the expansion approach. By imposing a revised set of boundary conditions along the interfaces, we first express the Green's functions in the Fourier-transformed domain in terms of a truncated series. Utilizing certain unique features in the transformed-domain Green's functions, each term in the series is further reduced to a line integral over the finite interval $[0, 2\pi]$, a remarkable reduction on the computational burden involved in the trimaterial Green's function evaluation. In Section 5, a numerical

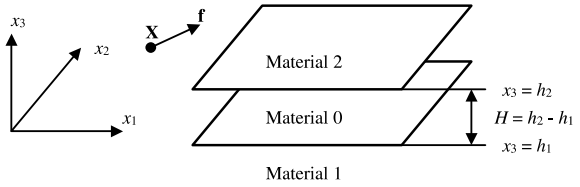

Fig. 1. A trimaterial system consisting of a plane-layer medium sandwiched by two opposite half-space media. The three media are in general distinct in materials properties. A Cartesian coordinate system is established with the x_3-axis perpendicular to the interfaces. The point force **f** is applied at an arbitrary source point **X**.

example is given to illustrate the efficiency and accuracy of the proposed expansion approach along with a convergence study. Finally, some conclusions are drawn in Section 6.

For the purpose of comparison, a direct 2D integral solution is also presented in the Appendix C for the trimaterial Green's functions. This solution is expressed as a sum of the homogeneous infinite-space solution and a complementary part. Since the infinite-space Green's function has an explicit expression, only the complementary part needs to be integrated numerically by a 2D quadrature.

2. Problem description

Let us consider a trimaterial composite made of a plate of uniform thickness H perfectly bonded by two half-space media, as shown in Fig. 1. A Cartesian coordinate system, (x_1, x_2, x_3), is attached to the composite with the x_3-axis perpendicular to the interfaces. Furthermore, the plate is labeled as material 0, the lower half-space as material 1, and the upper half-space as material 2. The three media are homogeneous, anisotropic, and linearly elastic, with distinct material properties in general. The Hooke's law for each material is given by

$$\sigma_{ij} = C_{ijkl}\varepsilon_{kl}, \tag{1}$$

where σ_{ij} is the stress tensor, ε_{kl} the strain tensor, and C_{ijkl} the elastic stiffness tensor consisting of 21 independent elements in general and different for different media. [1]

Let us further apply a point-force **f** to the trimaterial composite at a source point **X**. The equilibrium equation at a field point **x** can be written, in the absence of other body forces, as (Ting, 1996)

$$C_{ijkl}(\mathbf{x})u_{k,lj}(\mathbf{x}) = -f_i\delta(\mathbf{x}-\mathbf{X}), \tag{2}$$

where $\delta(\mathbf{x}-\mathbf{X})$ is the Dirac delta function, u_i is the displacement, and $,lj$ indicates the partial derivatives with respect to x_l and x_j sequentially. The condition of infinitesimal deformation is implied such that $\varepsilon_{kl} = (u_{k,l} + u_{l,k})/2$.

The perfectly bonded condition along the interfaces of the trimaterial are expressed as

$$\mathbf{u}_0 = \mathbf{u}_1 \quad \text{and} \quad \mathbf{t}_0 = \mathbf{t}_1, \ \text{at } x_3 = h_1, \tag{3}$$

$$\mathbf{u}_0 = \mathbf{u}_2 \quad \text{and} \quad \mathbf{t}_0 = \mathbf{t}_2, \ \text{at } x_3 = h_2, \tag{4}$$

[1] The standard notation system is used in the text. All Latin subscript indices range from 1 to 3. Greek subscript indices range from 1 to 2. A bold symbol for a tensor implies its subscript indices in the range from 1 to 3. Summation over repeated subscripts over their range is implied.

where $\mathbf{t} = \boldsymbol{\sigma}\mathbf{n}$ with $\mathbf{n} = (0,0,1)^{\mathrm{T}}$ in which T denotes *transpose* of a vector or matrix, h_1 and h_2 are the vertical levels of the lower and upper interfaces (Fig. 1), respectively, and the subscripts 0, 1, and 2 attached to the displacement and traction tensors indicate their association with the corresponding medium.

Furthermore, it is required that as $|\mathbf{x}|$ approaches infinity, the solution $\mathbf{u}$ vanishes, i.e.,

$$\lim_{|\mathbf{x}|\to\infty} u_k(\mathbf{x}) = 0. \tag{5}$$

This is called the radiation condition for a point-source solution in an infinite space.

This paper is, therefore, to solve the 3D response of the trimaterial composite to a point force $\mathbf{f}$ acting in any direction, as governed by Eq. (2), under the conditions, Eqs. (3)–(5). For this goal, it is sufficient to attain the fundamental solutions due to a unit point force acting in each direction of the axes. The fundamental solutions, also called Green's functions, are denoted by $u^*_{ji}(\mathbf{x};\mathbf{X})$ for displacement and $\sigma^*_{jki}(\mathbf{x};\mathbf{X})$ for stress. The last subscript i indicates the direction of the unit point force. Once these fundamental solutions are obtained, solutions at field point $\mathbf{x}$ due to the (arbitrary) $\mathbf{f}$ at source point $\mathbf{X}$ are readily obtained by

$$u_j(\mathbf{x}) = u^*_{ji}(\mathbf{x};\mathbf{X})f_i, \qquad \sigma_{jk}(\mathbf{x}) = \sigma^*_{jki}(\mathbf{x};\mathbf{X})f_i. \tag{6}$$

It is noted that while $\mathbf{u}$ is a vector, $\mathbf{u}^*$ is a tensor of the second rank. Similarly, $\boldsymbol{\sigma}^*$ is a tensor of one rank higher than $\boldsymbol{\sigma}$.

3. General solution in transformed domain

The approach we proposed is to first solve the trimaterial Green's function problem in the 2D Fourier-transformed domain in terms of the generalized Stroh's formalism, which is similar to those employed previously by Barnett and Lothe (1975), Ting (1996), and Pan and Yuan (2000) for the corresponding Green's function problem in an infinite, a semi-infinite, and a bimaterial space. The transformed-domain solution will then be inverted to obtain the physical-domain Green's function in the next section.

Now, let a 2D Fourier transform (y_1, y_2) be applied to the in-plane coordinates (x_1,x_2) of a physical quantity, for example for the displacement, as

$$\tilde{\boldsymbol{u}}_i(y_1,y_2,x_3) = \int\int u_i(x_1,x_2,x_3)\mathrm{e}^{\mathrm{i}y_\alpha x_\alpha}\,\mathrm{d}x_1\,\mathrm{d}x_2, \tag{7}$$

where e stands for the *exponential* function, and i over e denotes the unit of imaginary number, $\sqrt{-1}$. The integral limits are $(-\infty,\infty)$ for both coordinates. Therefore, in the Fourier-transformed domain, governing Eq. (2) becomes

$$C_{i\alpha k\beta}y_\alpha y_\beta\tilde{\boldsymbol{u}}_k + \mathrm{i}(C_{i\alpha k3} + C_{i3k\alpha})y_\alpha\tilde{\boldsymbol{u}}_{k,3} - C_{i3k3}\tilde{\boldsymbol{u}}_{k,33} = f_i\mathrm{e}^{\mathrm{i}y_\alpha X_\alpha}\delta(x_3 - X_3). \tag{8}$$

Solving this ordinary differential equation in x_3 with $\mathbf{f}$ being a unit force in the ith direction yields the fundamental solution for the Green's displacement in the jth direction in the transformed domain, $\tilde{\boldsymbol{u}}^*_{ji}$, as

$$\tilde{\mathbf{u}}^*(y_1,y_2,x_3;\mathbf{X}) = \mathrm{e}^{\mathrm{i}y_\alpha X_\alpha}\left\lfloor\tilde{\mathbf{u}}^{*(\infty)}(y_1,y_2,x_3;X_3) + \mathrm{i}\eta^{-1}\left(\overline{\mathbf{A}}\langle\mathrm{e}^{-\mathrm{i}\mathbf{p}\eta x_3}\rangle\mathbf{V} + \mathbf{A}\langle\mathrm{e}^{-\mathrm{i}\mathbf{p}\eta x_3}\rangle\mathbf{W}\right)\right\rfloor, \tag{9}$$

where the over bar denotes complex conjugate, (η,θ) are the polar coordinates related to (y_1,y_2) by $y_1 = \eta\cos\theta$ and $y_2 = \eta\sin\theta$, $\mathbf{V}$ and $\mathbf{W}$ are unknown tensors to be determined by the boundary conditions, and

$$\left\langle\mathrm{e}^{-\mathrm{i}\mathbf{p}\eta x_3}\right\rangle = \mathrm{diag}\left[\mathrm{e}^{-\mathrm{i}p_1\eta x_3}, \mathrm{e}^{-\mathrm{i}p_2\eta x_3}, \mathrm{e}^{-\mathrm{i}p_3\eta x_3}\right]. \tag{10}$$

with p_i and $\mathbf{A}$ being the eigenvalues and eigenmatrix of the generalized Stroh eigenproblem (Ting, 1996; Pan and Yuan, 2000). In addition, $\tilde{\mathbf{u}}^{*(\infty)}$ in Eq. (9) is the transformed Green's displacement in a homogeneous and infinite space with elastic properties identical to those in the medium in which the field point $\mathbf{x}$ is located while the point force $\mathbf{f}$ is applied at $\mathbf{X}$ (with $X_1 = 0$ and $X_2 = 0$ for simplicity), as given in Appendix A. Since the inverse of this Green's function, i.e., the physical-domain solution, has been derived explicitly by Ting and Lee (1997) and Tonon et al. (2001), the Fourier inverse transform needs to be carried out only for the complementary term in Eq. (9).

The eigenvalues p_i and eigenmatrix $\mathbf{A} = (\mathbf{a}_1, \mathbf{a}_2, \mathbf{a}_3)$ are related by the following Stroh eigenrelation in an oblique plane spanned by $(n_1 = \cos\theta,\ n_2 = \sin\theta,\ 0)^{\mathrm{T}}$, as

$$\left[\mathbf{Q} + p_i\left(\mathbf{R} + \mathbf{R}^{\mathrm{T}}\right) + p_i^2\mathbf{T}\right]\mathbf{a}_i = 0, \tag{11}$$

with

$$Q_{ik} = C_{i\alpha k\beta}n_\alpha n_\beta, \quad R_{ik} = C_{i\alpha k3}n_\alpha, \quad \text{and} \quad T_{ik} = C_{i3k3}. \tag{12}$$

It is seen that Eq. (11) produces six pairs of p_i and $\mathbf{a}_i$. However, only three pairs of them are independent. While $\mathbf{A}$ and p_i $(i = 1, 2, 3)$ are chosen to be the three independent pairs with Im $(p_i) > 0$, the other three pairs are their complex conjugates, i.e. $\overline{\mathbf{A}}$ and $\bar{p}_i$. Indeed, this fact has been reflected in the solution in Eq. (9), which is a linear combination of the six basic solutions. Also, it is worth mentioning that $\mathbf{A}$ and p_i are functions of materials constants and θ only, and the unknowns $\mathbf{V}$ and $\mathbf{W}$ are functions of η, θ, and X_3. These features are important in deriving the corresponding Green's stress by taking derivatives of $\tilde{\mathbf{u}}^*$, as will be seen below.

Let $\mathbf{s}$ be a vector containing the stress components in a plane parallel to the interface, namely, the in-plane stress vector. The combination of the traction (out-of-plane stress) vector $\mathbf{t}$ and the in-plane stress vector $\mathbf{s}$ then contains all the six stress components. Applying the constitutive law of the linear anisotropic elasticity (Eq. (1)), the corresponding fundamental stress solutions, $\mathbf{t}^*$ and $\mathbf{s}^*$, are then related to the derivatives of displacement, as

$$\mathbf{t}^* \equiv \left(\sigma^*_{13i}, \sigma^*_{23i}, \sigma^*_{33i}\right) = \left(C_{13kl}u^*_{ki,l}, C_{23kl}u^*_{ki,l}, C_{33kl}u^*_{ki,l}\right), \tag{13}$$

$$\mathbf{s}^* \equiv \left(\sigma^*_{11i}, \sigma^*_{12i}, \sigma^*_{22i}\right) = \left(C_{11kl}u^*_{ki,l}, C_{12kl}u^*_{ki,l}, C_{22kl}u^*_{ki,l}\right). \tag{14}$$

where the derivatives are taken with respect to the field point $\mathbf{x}$. Applying the 2D Fourier transform as defined in Eq. (7) to Eqs. (13) and (14), and making use of the general solution for the displacement (Eq. (9)), we then obtain the general solutions for $\mathbf{t}^*$ and $\mathbf{s}^*$, in the transformed domain, as

$$\tilde{\mathbf{t}}^*(y_1, y_2, x_3; \mathbf{X}) = \mathrm{e}^{\mathrm{i}y_\alpha X_\alpha}\lfloor\tilde{\mathbf{t}}^{*(\infty)}(y_1, y_2, x_3; X_3) + (\overline{\mathbf{B}}\langle\mathrm{e}^{-\mathrm{i}\mathbf{p}\eta x_3}\rangle\mathbf{V} + \mathbf{B}\langle\mathrm{e}^{-\mathrm{i}\mathbf{p}\eta x_3}\rangle\mathbf{W})\rfloor, \tag{15}$$

$$\tilde{\mathbf{s}}^*(y_1, y_2, x_3; \mathbf{X}) = \mathrm{e}^{\mathrm{i}y_\alpha X_\alpha}\lfloor\tilde{\mathbf{s}}^{*(\infty)}(y_1, y_2, x_3; X_3) + (\overline{\mathbf{C}}\langle\mathrm{e}^{-\mathrm{i}\mathbf{p}\eta x_3}\rangle\mathbf{V} + \mathbf{C}\langle\mathrm{e}^{-\mathrm{i}\mathbf{p}\eta x_3}\rangle\mathbf{W})\rfloor, \tag{16}$$

where $\tilde{\mathbf{t}}^{*(\infty)}$ and $\tilde{\mathbf{s}}^{*(\infty)}$, derived from $\tilde{\mathbf{u}}^{*(\infty)}$, are the Green's stresses in the transformed domain, as given in Appendix A. Again, the Fourier inverse transforms of these Green's functions, i.e., the physical-domain Green's stresses have been derived recently (Tonon et al., 2001), and therefore, the Fourier inverse transform needs to be carried out only for the complementary part of Eqs. (15) and (16).

Also in Eqs. (15) and (16), the matrices $\mathbf{B}$ and $\mathbf{C}$ are defined as $\mathbf{B} = (\mathbf{b}_1, \mathbf{b}_2, \mathbf{b}_3)$, and $\mathbf{C} = (\mathbf{c}_1, \mathbf{c}_2, \mathbf{c}_3)$, and are related to the matrix $\mathbf{A}$ by

$$\mathbf{b}_i = -\frac{1}{p_i}(\mathbf{Q} + p_i\mathbf{R})\mathbf{a}_i, \tag{17}$$

$$\mathbf{c}_i = \mathbf{D}_i\mathbf{a}_i, \tag{18}$$

with

$$D_{kli} = C_{1kl\alpha}n_\alpha + p_i C_{1kl3} \text{ for } k = 1,2, \quad \text{and} \quad D_{3li} = C_{22l\alpha}n_\alpha + p_i C_{22l3}. \tag{19}$$

where the matrix $\mathbf{C}$ is different from the fourth-rank elastic stiffness tensor C_{ijkl}. For clarity, the elastic stiffness tensor is always written in its component form in the text.

Once the transformed-domain solutions are found, the corresponding physical-domain solutions can be derived by the Fourier inverse transform. For instance, the physical-domain displacement can be expressed as

$$u_i(x_1,x_2,x_3) = \frac{1}{(2\pi)^2}\int\int \tilde{u}_i(y_1,y_2,x_3)\mathrm{e}^{-\mathrm{i}x_\alpha y_\alpha}\,\mathrm{d}y_1\,\mathrm{d}y_2, \tag{20}$$

where the integral limits in y_1 and y_2 are $(-\infty,\infty)$. The inverse transform may also be taken in the polar coordinates (η,θ) instead of (y_1,y_2), as

$$u_i(x_1,x_2,x_3) = \frac{1}{(2\pi)^2}\int\int \eta\tilde{u}_i(\eta,\theta,x_3)\mathrm{e}^{-\mathrm{i}\eta(x_1\cos\theta+x_2\sin\theta)}\,\mathrm{d}\eta\,\mathrm{d}\theta, \tag{21}$$

where $0<\eta<\infty$ and θ over a period of 2π. In terms of either expression, the integration, in general, needs to be evaluated numerically in the whole plane. Even with the fast Fourier transform (FFT) technique, the computational effort may still be very large, prohibiting an efficient numerical implementation of the boundary integral equation formulation using these Green's functions. Therefore, it would be very appreciable if the involved 2D integrals can be reduced analytically. This is achieved by the expansion approach presented in the next section.

4. Trimaterial Green's functions in physical domain

Motivated by the line-integral solution for the 3D Green's functions in anisotropic bimaterials (Pan and Yuan, 2000) and the image method (Yu and Sanday, 1993; Shou, 2000), we propose an expansion solution for the trimaterial Green's functions. It will be shown later that for such a complicated problem, i.e., general anisotropy with three material layers, the Green's functions can be expressed accurately by using only three or four terms with each of them being a simple line integral over $[0,2\pi]$.

To seek the trimaterial Green's functions by an expansion approach, we assume that the Green's functions in the Fourier-transformed domain can be expressed in the following series forms,

$$\begin{aligned}\tilde{\mathbf{u}}_0^*(y_1,y_2,x_3;\mathbf{X}) &= \mathrm{e}^{\mathrm{i}y_\alpha X_\alpha}\left(\tilde{\mathbf{u}}_0^{*(\infty)}(y_1,y_2,x_3;X_3) + \sum_{n=1}^{\infty}\tilde{\mathbf{u}}_0^{*(n)}(y_1,y_2,x_3;X_3)\right)\\ &= \mathrm{e}^{\mathrm{i}y_\alpha X_\alpha}\left(\tilde{\mathbf{u}}_0^{*(\infty)}(y_1,y_2,x_3;X_3) + \sum_{n=1}^{\infty}[\tilde{\mathbf{u}}_{01}^{*(n)}(y_1,y_2,x_3;X_3) + \tilde{\mathbf{u}}_{02}^{*(n)}(y_1,y_2,x_3;X_3)]\right),\end{aligned} \tag{22}$$

$$\begin{aligned}\tilde{\mathbf{t}}_0^*(y_1,y_2,x_3;\mathbf{X}) &= \mathrm{e}^{\mathrm{i}y_\alpha X_\alpha}\left(\tilde{\mathbf{t}}_0^{*(\infty)}(y_1,y_2,x_3;X_3) + \sum_{n=1}^{\infty}\tilde{\mathbf{t}}_0^{*(n)}(y_1,y_2,x_3;X_3)\right)\\ &= \mathrm{e}^{\mathrm{i}y_\alpha X_\alpha}\left(\tilde{\mathbf{t}}_0^{*(\infty)}(y_1,y_2,x_3;X_3) + \sum_{n=1}^{\infty}\left[\tilde{\mathbf{t}}_{01}^{*(n)}(y_1,y_2,x_3;X_3) + \tilde{\mathbf{t}}_{02}^{*(n)}(y_1,y_2,x_3;X_3)\right]\right),\end{aligned} \tag{23}$$

$$\tilde{\mathbf{s}}_0^*(y_1,y_2,x_3;\mathbf{X}) = \mathrm{e}^{\mathrm{i}y_\alpha X_\alpha}\left(\tilde{\mathbf{s}}_0^{*(\infty)}(y_1,y_2,x_3;X_3) + \sum_{n=1}^{\infty}\tilde{\mathbf{s}}_0^{*(n)}(y_1,y_2,x_3;X_3)\right)$$
$$= \mathrm{e}^{\mathrm{i}y_\alpha X_\alpha}\left(\tilde{\mathbf{s}}_0^{*(\infty)}(y_1,y_2,x_3;X_3) + \sum_{n=1}^{\infty}\left[\tilde{\mathbf{s}}_{01}^{*(n)}(y_1,y_2,x_3;X_3) + \tilde{\mathbf{s}}_{02}^{*(n)}(y_1,y_2,x_3;X_3)\right]\right), \tag{24}$$

for $h_1 < x_3 < h_2$ (material 0),

$$\tilde{\mathbf{u}}_1^*(y_1,y_2,x_3;\mathbf{X}) = \mathrm{e}^{\mathrm{i}y_\alpha X_\alpha}\left(\tilde{\mathbf{u}}_1^{*(\infty)}(y_1,y_2,x_3;X_3) + \sum_{n=1}^{\infty}\tilde{\mathbf{u}}_1^{*(n)}(y_1,y_2,x_3;X_3)\right), \tag{25}$$

$$\tilde{\mathbf{t}}_1^*(y_1,y_2,x_3;\mathbf{X}) = \mathrm{e}^{\mathrm{i}y_\alpha X_\alpha}\left(\tilde{\mathbf{t}}_1^{*(\infty)}(y_1,y_2,x_3;X_3) + \sum_{n=1}^{\infty}\tilde{\mathbf{t}}_1^{*(n)}(y_1,y_2,x_3;X_3)\right), \tag{26}$$

$$\tilde{\mathbf{s}}_1^*(y_1,y_2,x_3;\mathbf{X}) = \mathrm{e}^{\mathrm{i}y_\alpha X_\alpha}\left(\tilde{\mathbf{s}}_1^{*(\infty)}(y_1,y_2,x_3;X_3) + \sum_{n=1}^{\infty}\tilde{\mathbf{s}}_1^{*(n)}(y_1,y_2,x_3;X_3)\right), \tag{27}$$

for $x_3 < h_1$ (material 1), and

$$\tilde{\mathbf{u}}_2^*(y_1,y_2,x_3;\mathbf{X}) = \mathrm{e}^{\mathrm{i}y_\alpha X_\alpha}\left(\tilde{\mathbf{u}}_2^{*(\infty)}(y_1,y_2,x_3;X_3) + \sum_{n=1}^{\infty}\tilde{\mathbf{u}}_2^{*(n)}(y_1,y_2,x_3;X_3)\right), \tag{28}$$

$$\tilde{\mathbf{t}}_2^*(y_1,y_2,x_3;\mathbf{X}) = \mathrm{e}^{\mathrm{i}y_\alpha X_\alpha}\left(\tilde{\mathbf{t}}_2^{*(\infty)}(y_1,y_2,x_3;X_3) + \sum_{n=1}^{\infty}\tilde{\mathbf{t}}_2^{*(n)}(y_1,y_2,x_3;X_3)\right), \tag{29}$$

$$\tilde{\mathbf{s}}_2^*(y_1,y_2,x_3;\mathbf{X}) = \mathrm{e}^{\mathrm{i}y_\alpha X_\alpha}\left(\tilde{\mathbf{s}}_2^{*(\infty)}(y_1,y_2,x_3;X_3) + \sum_{n=1}^{\infty}\tilde{\mathbf{s}}_2^{*(n)}(y_1,y_2,x_3;X_3)\right), \tag{30}$$

for $x_3 > h_2$ (material 2).

In Eqs. (22)–(30),

$$\tilde{\mathbf{u}}_{01}^{*(n)}(y_1,y_2,x_3;X_3) = \mathrm{i}\eta^{-1}\overline{\mathbf{A}}_0\langle \mathrm{e}^{-\mathrm{i}\bar{\mathbf{p}}_0\eta x_3}\rangle\mathbf{V}_0^{(n)}, \tag{31}$$

$$\tilde{\mathbf{t}}_{01}^{*(n)}(y_1,y_2,x_3;X_3) = \overline{\mathbf{B}}_0\langle \mathrm{e}^{-\mathrm{i}\bar{\mathbf{p}}_0\eta x_3}\rangle\mathbf{V}_0^{(n)} = -\mathrm{i}\eta\overline{\mathbf{M}}_0\tilde{\mathbf{u}}_{01}^{*(n)}(y_1,y_2,x_3;X_3), \tag{32}$$

$$\tilde{\mathbf{s}}_{01}^{*(n)}(y_1,y_2,x_3;X_3) = \overline{\mathbf{C}}_0\langle \mathrm{e}^{-\mathrm{i}\bar{\mathbf{p}}_0\eta x_3}\rangle\mathbf{V}_0^{(n)} = -\mathrm{i}\eta\overline{\mathbf{N}}_0\tilde{\mathbf{u}}_{01}^{*(n)}(y_1,y_2,x_3;X_3), \tag{33}$$

$$\tilde{\mathbf{u}}_{02}^{*(n)}(y_1,y_2,x_3;X_3) = \mathrm{i}\eta^{-1}\mathbf{A}_0\langle \mathrm{e}^{-\mathrm{i}\mathbf{p}_0\eta x_3}\rangle\mathbf{W}_0^{(n)}, \tag{34}$$

$$\tilde{\mathbf{t}}_{02}^{*(n)}(y_1,y_2,x_3;X_3) = \mathbf{B}_0\langle \mathrm{e}^{-\mathrm{i}\mathbf{p}_0\eta x_3}\rangle\mathbf{W}_0^{(n)} = -\mathrm{i}\eta\mathbf{M}_0\tilde{\mathbf{u}}_{02}^{*(n)}(y_1,y_2,x_3;X_3), \tag{35}$$

$$\tilde{\mathbf{s}}_{02}^{*(n)}(y_1,y_2,x_3;X_3) = \mathbf{C}_0\langle \mathrm{e}^{-\mathrm{i}\mathbf{p}_0\eta x_3}\rangle\mathbf{W}_0^{(n)} = -\mathrm{i}\eta\mathbf{N}_0\tilde{\mathbf{u}}_{02}^{*(n)}(y_1,y_2,x_3;X_3), \tag{36}$$

$$\tilde{\mathbf{u}}_1^{*(n)}(y_1,y_2,x_3;X_3) = \mathrm{i}\eta^{-1}\mathbf{A}_1\langle \mathrm{e}^{-\mathrm{i}\mathbf{p}_1\eta x_3}\rangle\mathbf{W}_1^{(n)}, \tag{37}$$

$$\tilde{\mathbf{t}}_1^{*(n)}(y_1,y_2,x_3;X_3) = \mathbf{B}_1\langle \mathrm{e}^{-\mathrm{i}\mathbf{p}_1\eta x_3}\rangle\mathbf{W}_1^{(n)} = -\mathrm{i}\eta\mathbf{M}_1\tilde{\mathbf{u}}_1^{*(n)}(y_1,y_2,x_3;X_3), \tag{38}$$

$$\tilde{\mathbf{s}}_1^{*(n)}(y_1,y_2,x_3;X_3)=\mathbf{C}_1\langle \mathrm{e}^{-\mathrm{i}\tilde{\mathbf{p}}_1\eta x_3}\rangle\mathbf{W}_1^{(n)}=-\mathrm{i}\eta\mathbf{N}_1\tilde{\mathbf{u}}_1^{*(n)}(y_1,y_2,x_3;X_3), \tag{39}$$

$$\tilde{\mathbf{u}}_2^{*(n)}(y_1,y_2,x_3;X_3)=\mathrm{i}\eta^{-1}\overline{\mathbf{A}}_2\langle \mathrm{e}^{-\mathrm{i}\tilde{\mathbf{p}}_2\eta x_3}\rangle\mathbf{V}_2^{(n)}, \tag{40}$$

$$\tilde{\mathbf{t}}_2^{*(n)}(y_1,y_2,x_3;X_3)=\overline{\mathbf{B}}_2\langle \mathrm{e}^{-\mathrm{i}\tilde{\mathbf{p}}_2\eta x_3}\rangle\mathbf{V}_2^{(n)}=-\mathrm{i}\eta\overline{\mathbf{M}}_2\tilde{\mathbf{u}}_2^{*(n)}(y_1,y_2,x_3;X_3), \tag{41}$$

$$\tilde{\mathbf{s}}_2^{*(n)}(y_1,y_2,x_3;X_3)=\overline{\mathbf{C}}_2\langle \mathrm{e}^{-\mathrm{i}\tilde{\mathbf{p}}_2\eta x_3}\rangle\mathbf{V}_2^{(n)}=-\mathrm{i}\eta\overline{\mathbf{N}}_2\tilde{\mathbf{u}}_2^{*(n)}(y_1,y_2,x_3;X_3), \tag{42}$$

where $\mathbf{M}=\mathbf{B}\mathbf{A}^{-1}$, $\mathbf{N}=\mathbf{C}\mathbf{A}^{-1}$, and $\mathbf{V}_0^{(n)}$, $\mathbf{W}_0^{(n)}$, $\mathbf{W}_1^{(n)}$ and $\mathbf{V}_2^{(n)}$ are unknowns to be determined by the boundary conditions, Eqs. (3) and (4). Note that for $x_3<h_1$ and $x_3>h_2$, the radiation condition, Eq. (5) has been satisfied, retaining only one of the $\mathbf{V}$ and $\mathbf{W}$ as unknowns.

To find the unknown coefficients involved in Eqs. (31)–(42), we impose, instead of Eqs. (2) and (3), the following revised boundary conditions at $x_3=h_1$ and $x_3=h_2$, by truncating the series at a finite N and ignoring the remaining terms,

$$\tilde{\mathbf{u}}_0^{*(\infty)}(h_1)+\sum_{n=1}^{N-1}\left[\tilde{\mathbf{u}}_{01}^{*(n)}(h_1)+\tilde{\mathbf{u}}_{02}^{*(n)}(h_1)\right]+\tilde{\mathbf{u}}_{01}^{*(N)}(h_1)=\tilde{\mathbf{u}}_1^{*(\infty)}(h_1)+\sum_{n=1}^{N}\tilde{\mathbf{u}}_1^{*(n)}(h_1), \tag{43}$$

$$\tilde{\mathbf{t}}_0^{*(\infty)}(h_1)+\sum_{n=1}^{N-1}\left[\tilde{\mathbf{t}}_{01}^{*(n)}(h_1)+\tilde{\mathbf{t}}_{02}^{*(n)}(h_1)\right]+\tilde{\mathbf{t}}_{01}^{*(N)}(h_1)=\tilde{\mathbf{t}}_1^{*(\infty)}(h_1)+\sum_{n=1}^{N}\tilde{\mathbf{t}}_1^{*(n)}(h_1), \tag{44}$$

$$\tilde{\mathbf{u}}_0^{*(\infty)}(h_2)+\sum_{n=1}^{N-1}\left[\tilde{\mathbf{u}}_{01}^{*(n)}(h_2)+\tilde{\mathbf{u}}_{02}^{*(n)}(h_2)\right]+\tilde{\mathbf{u}}_{02}^{*(N)}(h_2)=\tilde{\mathbf{u}}_2^{*(\infty)}(h_2)+\sum_{n=1}^{N}\tilde{\mathbf{u}}_2^{*(n)}(h_2), \tag{45}$$

$$\tilde{\mathbf{t}}_0^{*(\infty)}(h_2)+\sum_{n=1}^{N-1}\left[\tilde{\mathbf{t}}_{01}^{*(n)}(h_2)+\tilde{\mathbf{t}}_{02}^{*(n)}(h_2)\right]+\tilde{\mathbf{t}}_{02}^{*(N)}(h_2)=\tilde{\mathbf{t}}_2^{*(\infty)}(h_2)+\sum_{n=1}^{N}\tilde{\mathbf{t}}_2^{*(n)}(h_2), \tag{46}$$

where the common arguments, y_1, y_2, and X_3, in the functions are omitted for simplicity and will be resumed as necessary for clarity.

Solving the set of Eqs. (43) and (44) and the set of Eqs. (45) and (46) respectively gives

$$\begin{aligned}(\mathbf{M}_1-\overline{\mathbf{M}}_0)\tilde{\mathbf{u}}_{01}^{*(N)}(h_1)&=\mathbf{M}_1\left(\tilde{\mathbf{u}}_1^{*(\infty)}(h_1)-\tilde{\mathbf{u}}_0^{*(\infty)}(h_1)\right)-\mathrm{i}\eta^{-1}\left(\tilde{\mathbf{t}}_1^{*(\infty)}(h_1)-\tilde{\mathbf{t}}_0^{*(\infty)}(h_1)\right)\\&\quad+\sum_{n=1}^{N-1}\left[(\overline{\mathbf{M}}_0-\mathbf{M}_1)\tilde{\mathbf{u}}_{01}^{*(n)}(h_1)+(\mathbf{M}_0-\mathbf{M}_1)\tilde{\mathbf{u}}_{02}^{*(n)}(h_1)\right],\end{aligned} \tag{47}$$

$$\begin{aligned}(\overline{\mathbf{M}}_2-\mathbf{M}_0)\tilde{\mathbf{u}}_{02}^{*(N)}(h_2)&=\overline{\mathbf{M}}_2\left(\tilde{\mathbf{u}}_2^{*(\infty)}(h_2)-\tilde{\mathbf{u}}_0^{*(\infty)}(h_2)\right)-\mathrm{i}\eta^{-1}\left(\tilde{\mathbf{t}}_2^{*(\infty)}(h_2)-\tilde{\mathbf{t}}_0^{*(\infty)}(h_2)\right)\\&\quad+\sum_{n=1}^{N-1}\left[(\overline{\mathbf{M}}_0-\overline{\mathbf{M}}_2)\tilde{\mathbf{u}}_{01}^{*(n)}(h_2)+(\mathbf{M}_0-\overline{\mathbf{M}}_2)\tilde{\mathbf{u}}_{02}^{*(n)}(h_2)\right],\end{aligned} \tag{48}$$

$$\begin{aligned}(\mathbf{M}_1-\overline{\mathbf{M}}_0)\sum_{n=1}^{N}\tilde{\mathbf{u}}_1^{*(n)}(h_1)&=\overline{\mathbf{M}}_0\left(\tilde{\mathbf{u}}_1^{*(\infty)}(h_1)-\tilde{\mathbf{u}}_0^{*(\infty)}(h_1)\right)-\mathrm{i}\eta^{-1}\left(\tilde{\mathbf{t}}_1^{*(\infty)}(h_1)-\tilde{\mathbf{t}}_0^{*(\infty)}(h_1)\right)\\&\quad+\sum_{n=1}^{N-1}(\mathbf{M}_0-\overline{\mathbf{M}}_0)\tilde{\mathbf{u}}_{02}^{*(n)}(h_1),\end{aligned} \tag{49}$$

$$(\overline{\mathbf{M}}_2-\mathbf{M}_0)\sum_{n=1}^{N}\tilde{\mathbf{u}}_2^{*(n)}(h_2)=\mathbf{M}_0\left(\tilde{\mathbf{u}}_2^{*(\infty)}(h_2)-\tilde{\mathbf{u}}_0^{*(\infty)}(h_2)\right)-\mathrm{i}\eta^{-1}\left(\tilde{\mathbf{t}}_2^{*(\infty)}(h_2)-\tilde{\mathbf{t}}_0^{*(\infty)}(h_2)\right)+\sum_{n=1}^{N-1}(\overline{\mathbf{M}}_0-\mathbf{M}_0)\tilde{\mathbf{u}}_{01}^{*(n)}(h_2). \tag{50}$$

Suppose that the above revised boundary conditions Eqs. (43)–(46) and the derived Eqs. (47)–(50) are valid for arbitrary $N(>0)$. Then, by subtracting two successive solutions, i.e., at N and $N-1$, Eqs. (47)–(50) can be rewritten in a recursive form as

$$\tilde{\mathbf{u}}_{01}^{*(1)}(h_1)=(\mathbf{M}_1-\overline{\mathbf{M}}_0)^{-1}\left[\mathbf{M}_1\left(\tilde{\mathbf{u}}_1^{*(\infty)}(h_1)-\tilde{\mathbf{u}}_0^{*(\infty)}(h_1)\right)-\mathrm{i}\eta^{-1}\left(\tilde{\mathbf{t}}_1^{*(\infty)}(h_1)-\tilde{\mathbf{t}}_0^{*(\infty)}(h_1)\right)\right], \tag{51}$$

$$\tilde{\mathbf{u}}_{02}^{*(1)}(h_2)=(\overline{\mathbf{M}}_2-\mathbf{M}_0)^{-1}\left[\overline{\mathbf{M}}_2\left(\tilde{\mathbf{u}}_2^{*(\infty)}(h_2)-\tilde{\mathbf{u}}_0^{*(\infty)}(h_2)\right)-\mathrm{i}\eta^{-1}\left(\tilde{\mathbf{t}}_2^{*(\infty)}(h_2)-\tilde{\mathbf{t}}_0^{*(\infty)}(h_2)\right)\right], \tag{52}$$

$$\tilde{\mathbf{u}}_{1}^{*(1)}(h_1)=(\mathbf{M}_1-\overline{\mathbf{M}}_0)^{-1}\left[\overline{\mathbf{M}}_0\left(\tilde{\mathbf{u}}_1^{*(\infty)}(h_1)-\tilde{\mathbf{u}}_0^{*(\infty)}(h_1)\right)-\mathrm{i}\eta^{-1}\left(\tilde{\mathbf{t}}_1^{*(\infty)}(h_1)-\tilde{\mathbf{t}}_0^{*(\infty)}(h_1)\right)\right], \tag{53}$$

$$\tilde{\mathbf{u}}_{2}^{*(1)}(h_2)=(\overline{\mathbf{M}}_2-\mathbf{M}_0)^{-1}\left[\mathbf{M}_0\left(\tilde{\mathbf{u}}_2^{*(\infty)}(h_2)-\tilde{\mathbf{u}}_0^{*(\infty)}(h_2)\right)-\mathrm{i}\eta^{-1}\left(\tilde{\mathbf{t}}_2^{*(\infty)}(h_2)-\tilde{\mathbf{t}}_0^{*(\infty)}(h_2)\right)\right]. \tag{54}$$

for the first order ($N=1$), and

$$\tilde{\mathbf{u}}_{01}^{*(N)}(h_1)=(\mathbf{M}_1-\overline{\mathbf{M}}_0)^{-1}(\mathbf{M}_0-\mathbf{M}_1)\tilde{\mathbf{u}}_{02}^{*(N-1)}(h_1), \tag{55}$$

$$\tilde{\mathbf{u}}_{02}^{*(N)}(h_2)=(\overline{\mathbf{M}}_2-\mathbf{M}_0)^{-1}(\overline{\mathbf{M}}_0-\overline{\mathbf{M}}_2)\tilde{\mathbf{u}}_{01}^{*(N-1)}(h_2), \tag{56}$$

$$\tilde{\mathbf{u}}_{1}^{*(N)}(h_1)=(\mathbf{M}_1-\overline{\mathbf{M}}_0)^{-1}(\mathbf{M}_0-\overline{\mathbf{M}}_0)\tilde{\mathbf{u}}_{02}^{*(N-1)}(h_1), \tag{57}$$

$$\tilde{\mathbf{u}}_{2}^{*(N)}(h_2)=(\overline{\mathbf{M}}_2-\mathbf{M}_0)^{-1}(\overline{\mathbf{M}}_0-\mathbf{M}_0)\tilde{\mathbf{u}}_{01}^{*(N-1)}(h_2), \tag{58}$$

for $N=2,3,\ldots,\infty$.

Finally, by substituting the above solutions into Eqs. (31), (34), (37) and (40), attaining the unknown tensors $\mathbf{V}_0^{(n)}$, $\mathbf{W}_0^{(n)}$, $\mathbf{W}_1^{(n)}$ and $\mathbf{V}_2^{(n)}$, and rearranging the results, the Nth-order solutions of the displacement in the transformed domain for arbitrary x_3 are obtained as

$$\tilde{\mathbf{u}}_0^{*(N)}(x_3)=\tilde{\mathbf{u}}_{01}^{*(N)}(x_3)+\tilde{\mathbf{u}}_{02}^{*(N)}(x_3),\quad \text{for } h_1<x_3<h_2, \tag{59}$$

with

$$\tilde{\mathbf{u}}_{01}^{*(N)}(x_3)=\overline{\mathbf{A}}_0\langle \mathrm{e}^{-\mathrm{i}\bar{\mathbf{p}}_0\eta(x_3-h_1)}\rangle\overline{\mathbf{A}}_0^{-1}\tilde{\mathbf{u}}_{01}^{*(N)}(h_1), \tag{59a}$$

$$\tilde{\mathbf{u}}_{02}^{*(N)}(x_3)=\mathbf{A}_0\left\langle \mathrm{e}^{-\mathrm{i}\mathbf{p}_0\eta(x_3-h_2)}\right\rangle\mathbf{A}_0^{-1}\tilde{\mathbf{u}}_{02}^{*(N)}(h_2), \tag{59b}$$

and

$$\tilde{\mathbf{u}}_1^{*(N)}(x_3)=\mathbf{A}_1\left\langle \mathrm{e}^{-\mathrm{i}\mathbf{p}_1\eta(x_3-h_1)}\right\rangle\mathbf{A}_1^{-1}\tilde{\mathbf{u}}_1^{*(N)}(h_1),\quad \text{for } x_3<h_1, \tag{60}$$

$$\tilde{\mathbf{u}}_2^{*(N)}(x_3)=\overline{\mathbf{A}}_2\langle \mathrm{e}^{-\mathrm{i}\bar{\mathbf{p}}_2\eta(x_3-h_2)}\rangle\overline{\mathbf{A}}_2^{-1}\tilde{\mathbf{u}}_2^{*(N)}(h_2),\quad \text{for } x_3>h_2, \tag{61}$$

for $N=1,2,\ldots,\infty$, with their values at $x_3=h_1$ or at $x_3=h_2$ being derived by the recursive Eqs. (51)–(58). Since the Green's functions at the root order, i.e. the infinite-space ones, are known, one can derive the

Green's functions at higher orders one by one. Also, by recalling the relationships of $\mathbf{t}^*$ and $\mathbf{s}^*$ to $\mathbf{u}^*$ in Eqs. (32), (33), (35), (36), (38), (39), (41) and (42), the stress vectors are obtained by multiplying the displacement solutions by $i\eta^{-1}$, and $\mathbf{M}$, $\mathbf{N}$ or their conjugates accordingly.

It is noted that these expansion solutions can be reduced to the existing homogeneous infinite-space or bimaterial solutions (Pan and Yuan, 2000) by letting the elastic stiffness tensors in all the three materials or two adjacent materials be identical correspondingly. Another interesting reduction is to let the elastic stiffness tensor in one of the half spaces be zero. This leads to a model for a finite thickness plate over a half space, with potential applications to thin film and coating related problems. Furthermore, these expansion solutions resemble the image-method solutions. For instance, the first term on the right-hand side of these equations (with a superscript (∞)) is the zero-order image (i.e., loading point itself), corresponding to the homogeneous infinite-space Green's function with source point at $(0,0,X_3)$. Since this Green's function has been derived explicitly in the physical-domain (Ting and Lee, 1997; Tonon et al., 2001), no inverse Fourier transforms need to be carried out for this term when the physical-domain value is needed. Similarly, the second term on the right-hand side of these equations (i.e., $N=1$) is the first-order image that corresponds to the bimaterial Green's functions made of materials 1 and 0, or of materials 0 and 2, respectively. The source points of these bimaterial Green's functions are the images of the actual source point $(0,0,X_3)$ across the interface planes $x_3=h_1$ and $x_3=h_2$ (Fig. 1). Once again, these bimaterial Green's functions in the physical domain have been derived recently by Pan and Yuan (2000), where only a regular line integral over $[0,\pi]$ is involved. Furthermore, it is observed that all other terms in the series expansion correspond to different orders of image and should also be reducible to a regular line integral.

The inverse transform-operator, Eq. (20) or (21), can now be applied to the above expansion solutions to find their counterparts in the physical domain, which unfortunately contain a 2D integral over the infinite plane. However, the expansion solutions embrace certain unique features that allow an analytical reduction of the integral dimensions in the inverse transform, similar to the bimaterial solutions (Pan and Yuan, 2000), as described below.

To reduce the integral dimensions, we first develop an explicit expansion solution in the transformed domain, term by term, rooted in the homogeneous infinite-space solution. Without loss of generality, we find, for instance, that the transformed displacement tensor can be written as a sum of terms with each term having the following form:

$$\tilde{\mathbf{u}}^{*(N)} = \sum i\eta^{-1}\mathbf{J}_{N+1}\left\langle e^{-i\mathbf{r}_N\eta}\right\rangle\mathbf{J}_N\cdots\left\langle e^{-i\mathbf{r}_n\eta}\right\rangle\mathbf{J}_n\cdots\left\langle e^{-i\mathbf{r}_0\eta}\right\rangle\mathbf{J}_0, \tag{62}$$

for displacement, and

$$\tilde{\mathbf{t}}^{*(N)} = \sum \mathbf{J}_{N+1}\left\langle e^{-i\mathbf{r}_N\eta}\right\rangle\mathbf{J}_N\cdots\left\langle e^{-i\mathbf{r}_n\eta}\right\rangle\mathbf{J}_n\cdots\left\langle e^{-i\mathbf{r}_0\eta}\right\rangle\mathbf{J}_0, \tag{63}$$

for traction tensor and the same for in-plane stress tensor $\mathbf{s}^*$. In Eqs. (62) and (63), the tensors $\mathbf{J}_n(\theta)$ and vectors $\mathbf{r}_n(\theta)$ are independent of η but functions of θ. It is also remarked that the explicit expressions for these tensors and vectors depend also on the relative location of the source and field points, and therefore are very complicated and very lengthy. However, to illustrate the derivation and the features of these expressions, the explicit expression for the displacement vector (62) is given in Appendix B when both the source and field points are in the plate (i.e., in material 0).

Inserting expressions (62) and (63) multiplied by $e^{i\gamma_\alpha X_\alpha}$ into the inverse-transform operator, Eq. (21), gives

$$\begin{aligned}\mathbf{u}^{*(N)} &= \frac{1}{(2\pi)^2}\int\int \eta\tilde{\mathbf{u}}^{*(N)}e^{i\gamma_\alpha(X_\alpha-x_\alpha)}\,d\eta\,d\theta \\ &= \sum\frac{1}{(2\pi)^2}\int\int i\mathbf{J}_{N+1}\left\langle e^{-i\mathbf{r}_N\eta}\right\rangle\mathbf{J}_N\cdots\left\langle e^{-i\mathbf{r}_n\eta}\right\rangle\mathbf{J}_n\cdots\left\langle e^{-i\mathbf{r}_0\eta}\right\rangle\mathbf{J}_0e^{i\gamma_\alpha(X_\alpha-x_\alpha)}\,d\eta\,d\theta,\end{aligned} \tag{64}$$

for the displacement $\mathbf{u}^*$, and

$$\mathbf{t}^{*(N)} = \frac{1}{(2\pi)^2}\int\int \eta\tilde{\mathbf{t}}^{*(N)} e^{iy_\alpha(X_\alpha - x_\alpha)}\,d\eta\,d\theta$$
$$= \sum\frac{1}{(2\pi)^2}\int\int \eta\mathbf{J}_{N+1}\langle e^{-i\mathbf{r}_N\eta}\rangle\mathbf{J}_N\cdots\langle e^{-i\mathbf{r}_n\eta}\rangle\mathbf{J}_n\cdots\langle e^{-i\mathbf{r}_0\eta}\rangle\mathbf{J}_0 e^{iy_\alpha(X_\alpha - x_\alpha)}\,d\eta\,d\theta, \tag{65}$$

for the traction $\mathbf{t}^*$, with a similar expression for the in-plane stress $\mathbf{s}^*$. In Eqs. (64) and (65), the integral dimension limits in the polar coordinates are $0 < \eta < \infty$ and θ over a period of 2π.

With the transformed Green's displacement and stress being written as the multiplication of a series of exponential functions of η and a factor of η, as shown in Eqs. (64) and (65), it is seen now that the double integrals involved are reducible to a 1D integral by carrying out the integral in η over $(0, \infty)$. The reduced integrals are given by

$$u_{ji}^{*(N)} = \sum\frac{1}{(2\pi)^2}\oint_{2\pi} G_{ji}\left(\frac{1}{s} + i\delta(s)\right)d\theta, \tag{66}$$

$$t_{ji}^{*(N)} = \sum\frac{1}{(2\pi)^2}\oint_{2\pi} G_{ji}\left(-\frac{1}{s^2} + i\delta'(s)\right)d\theta, \tag{67}$$

where $\delta(k)$ is the Dirac delta, and the prime indicates the first derivative, with

$$G_{ji} = \left(J_{jk_{N+1}}\right)_{N+1}\left(J_{k_{N+1}k_N}\right)_N\cdots\left(J_{k_{n+1}k_n}\right)_n\cdots(J_{k_1 i})_0, \tag{68}$$

$$s = \left(r_{k_{N+1}}\right)_N + \cdots\left(r_{k_{n+1}}\right)_n + \cdots(r_{k_1})_0 - ((X_1 - x_1)\cos\theta + (X_2 - x_2)\sin\theta). \tag{69}$$

Note that the in-plane stress $\mathbf{s}^*$ has a similar expression as for $\mathbf{t}^*$ and that $\mathbf{u}^*$, $\mathbf{t}^*$ and $\mathbf{s}^*$ do not share the same G_{ji} and s. The finite-integral terms in Eqs. (66) and (67) exist when $s = 0$, in the situation when the source and field points are on the same interface plane. A detailed interfacial solution for a bimaterial system can be found in Pan and Yang (submitted for publication).

In summary, with the expansion approach we proposed, the trimaterial Green's functions in the physical domain are derived in terms of an infinite series. It is shown that each term in the series, excluding the infinite-space term that can be treated analytically, can be expressed by a simple line integral over the interval $[0, 2\pi]$. Therefore, the trimaterial Green's functions obtained with the expansion approach should be able to reduce the computational time substantially as compared to the direct 2D integral method given in the Appendix C. This is verified and illustrated numerically in the next section.

5. Numerical examples

Before presenting numerical examples for the trimaterial Green's function, we first remark that our trimaterial Green's functions have been verified for various reduced cases. These include a homogeneous infinite space where the infinite space is divided artificially into three identical materials, and a bimaterial space where one of the half spaces is artificially modeled as a plate of uniform thickness over a half space, both with identical elastic properties. It is found that for these reduced cases, the present trimaterial Green's functions predict the same results as those obtained by Tonon et al. (2001) for the infinite space and by Pan and Yuan (2000) for the bimaterial case. Also, for the true trimaterial systems, a dilatation example in Yu and Sanday (1993) has been checked and we found that our solution is in consistent with that presented in Yu and Sanday (1993). Furthermore, the numerical examples for the trimaterial system given below are

Table 1
Elastic constants of material 1 (reduced C_{ijkl})

1.45	0.99	0.96	−0.02	−0.31177	−0.15588
	1.85	0.96	−0.22	−0.10392	−0.19052
		1.28	−0.16	−0.27713	0
			0.32	0	−0.10392
				0.32	−0.02
					0.35

based on both the series and direct 2D solutions, and therefore serve, additionally, as mutual checks for the direct 2D solution as well as the series solution.

In the following, a trimaterial system, made of two half-space solids perfectly bonded by an adhesive with thickness equal to one unit (i.e. $H = 1$), is chosen in the numerical study. The half-space solids are anisotropic with their elastic constants being given in Table 1 (Tonon et al., 2001) and Table 2 (Pan et al., 2001), respectively. The adhesive material is assumed to be isotropic, with Young's modulus $E = 0.7464$, and Poison's ratio $v = 0.34$. As an example, the source point $\mathbf{X}$ is fixed in the middle plane of the adhesive layer. An adaptive quadrature scheme was applied to compute numerically the physical-domain Green's functions by the expansion approach as well as by the direct 2D integral method in the Appendix A. The computational time required by the expansion approach with two or three terms was found to be less than 10% of that needed by the direct 2D integral method.

Figs. 2–4 show the variations of the Green's displacement, traction and in-plane stress components with the field coordinate x_3 along a vertical line at $(x_1 = 0.5,\ x_2 = 0,\ x_3)$ due to a point force in the x_1-, x_2-, and x_3-directions, respectively. In these figures, the "true solutions" indicate those obtained by the direct 2D integral method and "1-term, 2-term, and 3-term solutions" are those by the expansion approach with one, two, and three successive terms of the series respectively. It is obvious that a good approximation has been obtained with only two or three terms, particularly, for the traction and stress components. Furthermore, these results show clearly the influence of the material layering, as well as material anisotropy, on the Green's displacement and stress components. For instance, the true solution by the direct 2D integral shows that the displacement $\mathbf{u}^*$ and traction $\mathbf{t}^*$ are continuous across both interfaces at $x_3 - (h_1 + h_2)/2 = -0.5$ and 0.5. However, at these interfaces, obvious kinks in these curves are observed, indicating discontinuity in their derivatives in the x_3-direction. On the other hand, the in-plane stress components $\mathbf{s}^*$ experience clear discontinuities across the interfaces, due to the mismatch of materials properties between the media.

To show a convergence of the expansion approach with increasing number of successive terms, the component, u^*_{33}, its expansion solution badly deviates from the true value (Fig. 2), is reexamined in detail. Fig. 5 shows the variation of this component with x_1 along a horizontal line $(x_1,\ x_2 = 0,\ x_3 - (h_1 + h_2)/2 = 0)$ (a), the absolute (b), and relative (c) errors for one to four terms. Based on these figures as well as the previous figures, it is demonstrated that the expansion solutions converge with increasing number of successive terms, and with only three or four terms, a satisfactory solution can be achieved (i.e., within an error of 5%). The absolute error becomes smaller when the field point is farther away from the source point

Table 2
Elastic constants of material 2 (reduced C_{ijkl})

1.03520185	0.052384	0.052384	0	0	0
	0.115377	0.040527	0	0	0
		0.115377	0	0	0
			0.033333	0	0
				0.033333	0
					0.033333

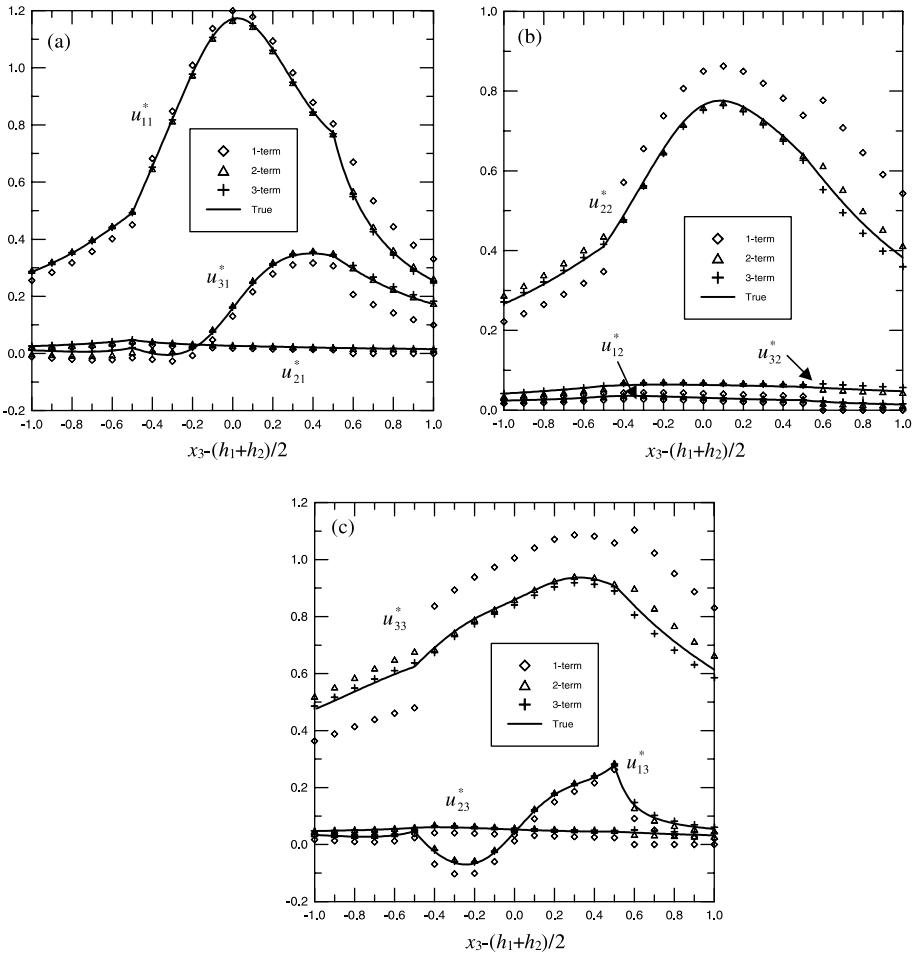

Fig. 2. Variation of the trimaterial Green's displacement components along a vertical line $(x_1 = 0.5,\ x_2 = 0,\ x_3)$ due to a point force applied at $(x_1 = 0,\ x_2 = 0,\ x_3 = (h_1 + h_2)/2)$ in the (a) x_1-direction; (b) x_2-direction; and (c) x_3-direction. The "true solution" represented by solid line is the solution obtained by the direct 2D integral method and "1-term, 2-term, and 3-term solutions" are those by the truncated expansion approach with one, two, and three successive terms of the series respectively.

(Fig. 5b) while the relative error becomes larger. The reason is that the absolute value of the solution decays with distance but the influence of the truncated terms (images) becomes more and more comparable to that of the original source and the first few images (Fig. 5c). Note that the convergence with increasing number of successive terms is not monotonic, as shown in Fig. 5. The errors are very small in the approximation with the first two and the first four terms, while they are relatively large with the first three terms.

In addition, we have studied a few other systems of trimaterials with different combinations of materials. The results showed similar behaviors to what were observed in the previous system. Besides, the smaller the dissimilarity between the materials, the smaller the truncated series terms to converge. As extreme cases, when the three materials are all the same, the trimaterial composite reduces to a homogeneous infinite space. When one of the half-space media is the same as the plate medium, the trimaterial composite reduces to a bimaterial composite (Pan and Yuan, 2000), where the first expansion term is sufficient to describe the complementary part due to the single interface.

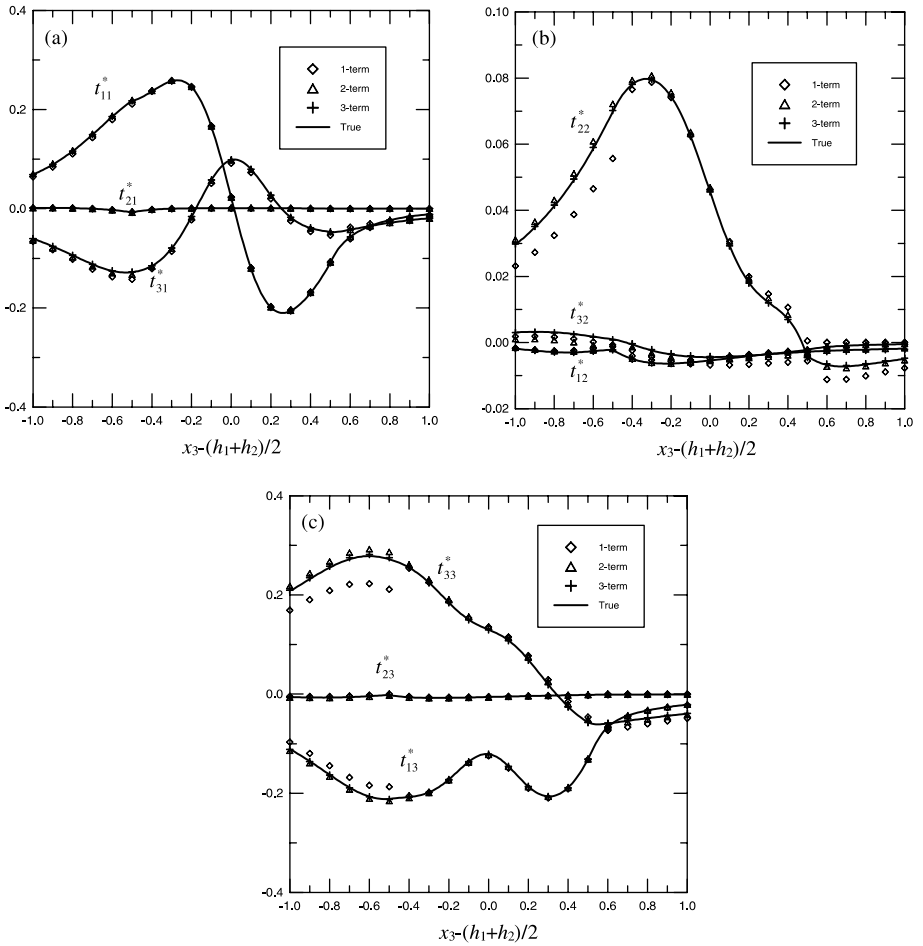

Fig. 3. Variation of the trimaterial Green's out-of-plane stress components along a vertical line $(x_1 = 0.5,\ x_2 = 0,\ x_3)$ due to a point force applied at $(x_1 = 0,\ x_2 = 0,\ x_3 = (h_1 + h_2)/2)$ in the (a) x_1-direction; (b) x_2-direction; and (c) x_3-direction. The "true solution" represented by solid line is the solution obtained by the direct 2D integral method and "1-term, 2-term, and 3-term solutions" are those by the truncated expansion approach with one, two, and three successive terms of the series respectively.

6. Conclusions

Three-dimensional elastostatic Green's functions in anisotropic trimaterials have been derived, *for the first time*, by applying the generalized Stroh's formalism and Fourier transforms. The Green's functions are expressed as a finite series summation with each term having a clear physical meaning that resembles the image method. In particular, the first term corresponds to the infinite-space Green's function, which has an explicit-form solution (Ting and Lee, 1997; Tonon et al., 2001), and the second term corresponds to the bimaterial solution developed previously by Pan and Yuan (2000). The most remarkable feature of the present solution is that every term of the series can be expressed by a simple and regular line integral over the finite interval $[0, 2\pi]$, resembling one image of the source. The solution developed is practically very useful since only two or three terms are required in most cases representing fiber composites and materials as examined by the authors. Furthermore, by partitioning the trimaterial Green's function into a full-space solution and a complementary part, the line integral involves only regular functions if the singularity is

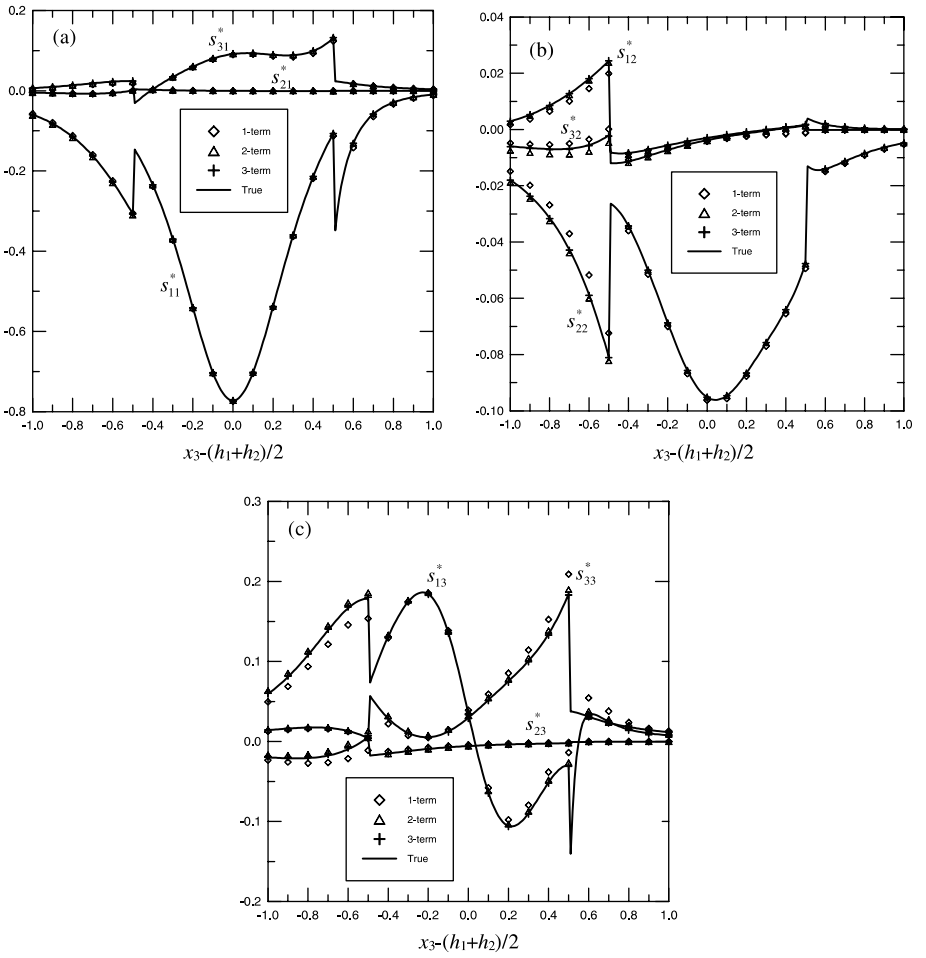

Fig. 4. Variation of the trimaterial Green's in-plane stress components along a vertical line ($x_1 = 0.5,\ x_2 = 0,\ x_3$) due to a point force applied at ($x_1 = 0,\ x_2 = 0,\ x_3 = (h_1 + h_2)/2$) in the (a) x_1-direction; (b) x_2-direction; and (c) x_3-direction. The "true solution" represented by solid line is the solution obtained by the direct 2D integral method and "1-term, 2-term, and 3-term solutions" are those by the truncated expansion approach with one, two, and three successive terms of the series respectively.

within one of the three material, being treated analytically owning to the explicit expression of the full-space solution (Ting and Lee, 1997; Tonon et al., 2001). When the singularity is on the interface, which occurs if the field and source points are both on the same interface, the involved singularity is handled with the interfacial Green's functions (Pan and Yang, submitted for publication).

Since the trimaterial model includes many practical physical models as its special cases, such as a thin film on a substrate, a simple finite plate, and bimaterial, the present solution is of great interests in these areas where the physical models need to be analyzed numerically. In particular, the present trimaterial Green's function can be directly applied to the study of quantum-dot growth in modern semiconductor devices. The numerical examples presented in this paper have clearly shown the efficiency and accuracy of the expansion method in comparison to the direct 2D integral solution. The results also show the significant influence of material layering (or stacking sequences) on the displacement and stress fields. The present study, using an adaptive quadrature scheme, showed that the computational time for the calculation of the

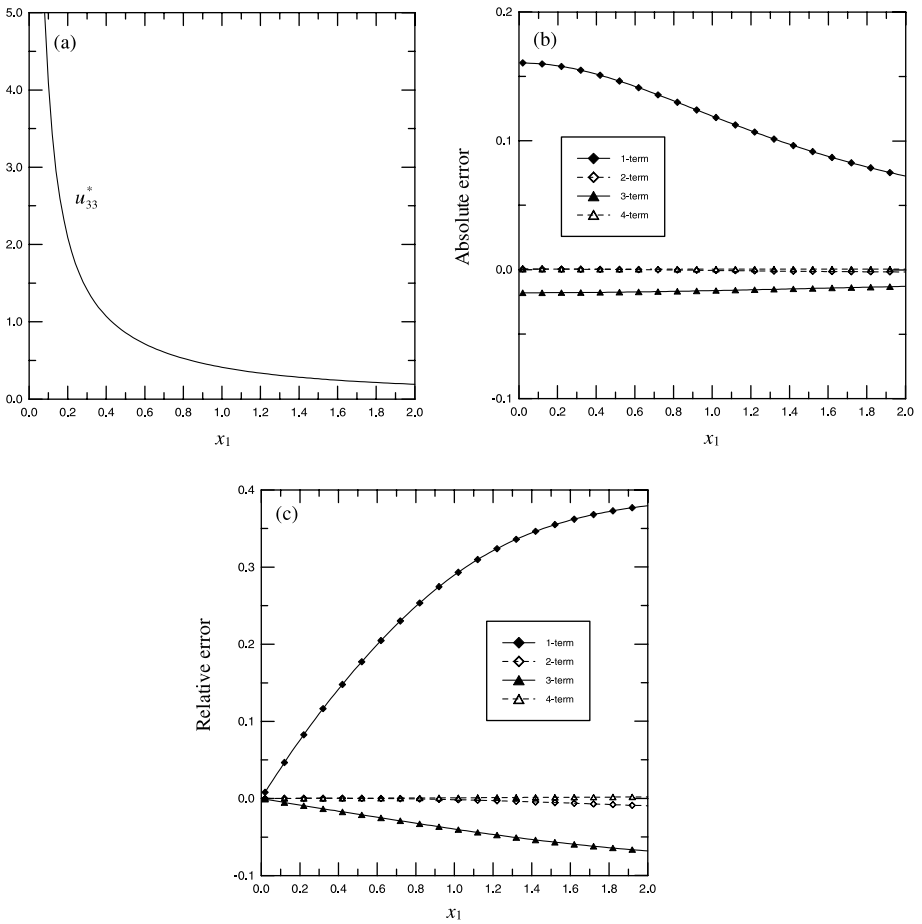

Fig. 5. Variation of the trimaterial Green's displacement component u_{33}^* in (a), its absolute error in (b), and its relative error in (c), with x_1 along a line at $(x_1,\ x_2 = 0,\ x_3 - (h_1 + h_2)/2 = 0)$.

physical-domain Green's functions based on the expansion approach can be substantially reduced as compared to the direct 2D integral approach.

Acknowledgements

The authors would like to thank both reviewers for their constructive comments. This project is supported in part by the AFOSR under grant no. F33615-97-C-5089 with Dr. Richard Hall being the project manager.

Appendix A. Transformed Green's displacement and stress in an infinite homogeneous space

The transformed Green's displacement and stress in an infinite homogeneous space due to a unit axial point force at $(X_1 = 0,\ X_2 = 0,\ X_3)$, $\tilde{\mathbf{u}}^{*(\infty)}$, $\tilde{\mathbf{t}}^{*(\infty)}$ and $\tilde{\mathbf{s}}^{*(\infty)}$ are given by

$$\tilde{\mathbf{u}}^{*(\infty)}(y_1,y_2,x_3;X_3)=\mathrm{i}\eta^{-1}\begin{cases}\mathbf{A}\langle \mathrm{e}^{-\mathrm{i}\mathbf{p}\eta(x_3-X_3)}\rangle\mathbf{A}^{-1}\left(\mathbf{B}\mathbf{A}^{-1}-\overline{\mathbf{B}}\overline{\mathbf{A}}^{-1}\right)^{-1}, & x_3<X_3,\\ \overline{\mathbf{A}}\langle \mathrm{e}^{-\mathrm{i}\bar{\mathbf{p}}\eta(x_3-X_3)}\rangle\overline{\mathbf{A}}^{-1}\left(\mathbf{B}\mathbf{A}^{-1}-\overline{\mathbf{B}}\overline{\mathbf{A}}^{-1}\right)^{-1}, & x_3>X_3,\end{cases} \tag{A.1}$$

$$\tilde{\mathbf{t}}^{*(\infty)}(y_1,y_2,x_3;X_3)=\begin{cases}\mathbf{B}\langle \mathrm{e}^{-\mathrm{i}\mathbf{p}\eta(x_3-X_3)}\rangle\mathbf{A}^{-1}\left(\mathbf{B}\mathbf{A}^{-1}-\overline{\mathbf{B}}\overline{\mathbf{A}}^{-1}\right)^{-1}, & x_3<X_3,\\ \overline{\mathbf{B}}\langle \mathrm{e}^{-\mathrm{i}\bar{\mathbf{p}}\eta(x_3-X_3)}\rangle\overline{\mathbf{A}}^{-1}\left(\mathbf{B}\mathbf{A}^{-1}-\overline{\mathbf{B}}\overline{\mathbf{A}}^{-1}\right)^{-1}, & x_3>X_3,\end{cases} \tag{A.2}$$

$$\tilde{\mathbf{s}}^{*(\infty)}(y_1,y_2,x_3;X_3)=\begin{cases}\mathbf{C}\langle \mathrm{e}^{-\mathrm{i}\mathbf{p}\eta(x_3-X_3)}\rangle\mathbf{A}^{-1}\left(\mathbf{B}\mathbf{A}^{-1}-\overline{\mathbf{B}}\overline{\mathbf{A}}^{-1}\right)^{-1}, & x_3<X_3,\\ \overline{\mathbf{C}}\langle \mathrm{e}^{-\mathrm{i}\bar{\mathbf{p}}\eta(x_3-X_3)}\rangle\overline{\mathbf{A}}^{-1}\left(\mathbf{B}\mathbf{A}^{-1}-\overline{\mathbf{B}}\overline{\mathbf{A}}^{-1}\right)^{-1}, & x_3>X_3.\end{cases} \tag{A.3}$$

Appendix B. Explicit expressions of expansion terms in the trimaterial Green's function

A complete description of the explicit expressions for the trimaterial Green's function expansion terms (Eqs. (62) and (63)) is lengthy and redundant. However, as an example, we derive below the explicit expression for the Green's displacement with the source and field points both in the middle layer ($h_1 < X_3 < h_2,\ h_1 < x_3 < h_2$), corresponding to Eq. (59) inserted with Eqs. (51), (52), (55) and (56).

In this case ($h_1 < X_3 < h_2$, $h_1 < x_3 < h_2$), for $N = 1$, Eqs. (51) and (52) becomes

$$\tilde{\mathbf{u}}_{01}^{*(1)}(h_1)=\left(\mathbf{M}_1-\overline{\mathbf{M}}_0\right)^{-1}(\mathbf{M}_0-\mathbf{M}_1)\tilde{\mathbf{u}}_0^{*(\infty)}(h_1), \tag{B.1}$$

$$\tilde{\mathbf{u}}_{02}^{*(1)}(h_2)=\left(\overline{\mathbf{M}}_2-\mathbf{M}_0\right)^{-1}(\overline{\mathbf{M}}_0-\overline{\mathbf{M}}_2)\tilde{\mathbf{u}}_0^{*(\infty)}(h_2), \tag{B.2}$$

where $\tilde{\mathbf{u}}_0^{*(\infty)}(h_1)$ and $\tilde{\mathbf{u}}_0^{*(\infty)}(h_2)$ are given by substituting $x_3 = h_1$ and $x_3 = h_2$ in Eq. (A.1) respectively. Thus, substituting Eqs. (B.1) and (B.2) in Eqs. (59a) and (59b) respectively yields

$$\tilde{\mathbf{u}}_{01}^{*(1)}(x_3)=\overline{\mathbf{A}}_0\left\langle \mathrm{e}^{-\mathrm{i}\bar{\mathbf{p}}_0\eta(x_3-h_1)}\right\rangle\overline{\mathbf{A}}_0^{-1}\left(\mathbf{M}_1-\overline{\mathbf{M}}_0\right)^{-1}(\mathbf{M}_0-\mathbf{M}_1)\tilde{\mathbf{u}}_0^{*(\infty)}(h_1), \tag{B.3}$$

$$\tilde{\mathbf{u}}_{02}^{*(1)}(x_3)=\mathbf{A}_0\langle \mathrm{e}^{-\mathrm{i}\mathbf{p}_0\eta(x_3-h_2)}\rangle\mathbf{A}_0^{-1}\left(\overline{\mathbf{M}}_2-\mathbf{M}_0\right)^{-1}\left(\overline{\mathbf{M}}_0-\overline{\mathbf{M}}_2\right)\tilde{\mathbf{u}}_0^{*(\infty)}(h_2). \tag{B.4}$$

The higher order terms are then derived consecutively; for example, the second-order term is derived below.

For $N = 2$, first, substituting $x_3 = h_1$ and $x_3 = h_2$ in Eqs. (B.3) and (B.4) yields

$$\tilde{\mathbf{u}}_{01}^{*(1)}(h_2)=\overline{\mathbf{A}}_0\langle \mathrm{e}^{-\mathrm{i}\bar{\mathbf{p}}_0\eta H}\rangle\overline{\mathbf{A}}_0^{-1}\left(\mathbf{M}_1-\overline{\mathbf{M}}_0\right)^{-1}(\mathbf{M}_0-\mathbf{M}_1)\tilde{\mathbf{u}}_0^{*(\infty)}(h_1), \tag{B.5}$$

$$\tilde{\mathbf{u}}_{02}^{*(1)}(h_1)=\mathbf{A}_0\langle \mathrm{e}^{\mathrm{i}\mathbf{p}_0\eta H}\rangle\mathbf{A}_0^{-1}\left(\overline{\mathbf{M}}_2-\mathbf{M}_0\right)^{-1}\left(\overline{\mathbf{M}}_0-\overline{\mathbf{M}}_2\right)\tilde{\mathbf{u}}_0^{*(\infty)}(h_2). \tag{B.6}$$

Further substituting Eqs. (B.5) and (B.6) in Eqs. (55) and (56) respectively yields

$$\tilde{\mathbf{u}}_{01}^{*(2)}(h_1)=\left(\mathbf{M}_1-\overline{\mathbf{M}}_0\right)^{-1}(\mathbf{M}_0-\mathbf{M}_1)\mathbf{A}_0\langle \mathrm{e}^{\mathrm{i}\mathbf{p}_0\eta H}\rangle\mathbf{A}_0^{-1}\left(\overline{\mathbf{M}}_2-\mathbf{M}_0\right)^{-1}\left(\overline{\mathbf{M}}_0-\overline{\mathbf{M}}_2\right)\tilde{\mathbf{u}}_0^{*(\infty)}(h_2), \tag{B.7}$$

$$\tilde{\mathbf{u}}_{02}^{*(2)}(h_2)=\left(\overline{\mathbf{M}}_2-\mathbf{M}_0\right)^{-1}\left(\overline{\mathbf{M}}_0-\overline{\mathbf{M}}_2\right)\overline{\mathbf{A}}_0\langle \mathrm{e}^{-\mathrm{i}\bar{\mathbf{p}}_0\eta H}\rangle\overline{\mathbf{A}}_0^{-1}\left(\mathbf{M}_1-\overline{\mathbf{M}}_0\right)^{-1}(\mathbf{M}_0-\mathbf{M}_1)\tilde{\mathbf{u}}_0^{*(\infty)}(h_1). \tag{B.8}$$

Therefore, the second-order terms are obtained as

$$\tilde{\mathbf{u}}_{01}^{*(2)}(x_3) = \overline{\mathbf{A}}_0\langle e^{-i\bar{\mathbf{p}}_0\eta(x_3-h_1)}\rangle\overline{\mathbf{A}}_0^{-1}\left(\mathbf{M}_1-\overline{\mathbf{M}}_0\right)^{-1}(\mathbf{M}_0-\mathbf{M}_1)\mathbf{A}_0\langle e^{i\mathbf{p}_0\eta H}\rangle\mathbf{A}_0^{-1}\left(\overline{\mathbf{M}}_2-\mathbf{M}_0\right)^{-1}\left(\overline{\mathbf{M}}_0-\overline{\mathbf{M}}_2\right)\tilde{\mathbf{u}}_0^{*(\infty)}(h_2), \tag{B.9}$$

$$\tilde{\mathbf{u}}_{02}^{*(2)}(x_3) = \mathbf{A}_0\langle e^{-i\mathbf{p}_0\eta(x_3-h_2)}\rangle\mathbf{A}_0^{-1}\left(\overline{\mathbf{M}}_2-\mathbf{M}_0\right)^{-1}\left(\overline{\mathbf{M}}_0-\overline{\mathbf{M}}_2\right)\overline{\mathbf{A}}_0\langle e^{-i\bar{\mathbf{p}}_0\eta H}\rangle\overline{\mathbf{A}}_0^{-1}\left(\mathbf{M}_1-\overline{\mathbf{M}}_0\right)^{-1}(\mathbf{M}_0-\mathbf{M}_1)\tilde{\mathbf{u}}_0^{*(\infty)}(h_1). \tag{B.10}$$

The following higher order terms may be derived in the same procedure. For this case of $h_1 < X_3 < h_2$ and $h_1 < x_3 < h_2$, we found that all the terms can be expressed in the following condensed forms:

$$\tilde{\mathbf{u}}_{01}^{*(N)}(x_3) = \overline{\mathbf{A}}_0\langle e^{-i\bar{\mathbf{p}}_0\eta(x_3-h_1)}\rangle[\mathbf{L}_1\langle e^{i\mathbf{p}_0\eta H}\rangle\mathbf{L}_2\langle e^{-i\bar{\mathbf{p}}_0\eta H}\rangle]^m\begin{cases}\mathbf{L}_1\mathbf{A}_0^{-1}\tilde{\mathbf{u}}_0^{*(\infty)}(h_1) & \text{if } N \text{ is odd;}\\ \mathbf{L}_1\langle e^{i\mathbf{p}_0\eta H}\rangle\mathbf{L}_2\overline{\mathbf{A}}_0^{-1}\tilde{\mathbf{u}}_0^{*(\infty)}(h_2) & \text{if } N \text{ is even,}\end{cases} \tag{B.11}$$

$$\tilde{\mathbf{u}}_{02}^{*(N)}(x_3) = \mathbf{A}_0\langle e^{-i\mathbf{p}_0\eta(x_3-h_2)}\rangle[\mathbf{L}_2\langle e^{-i\bar{\mathbf{p}}_0\eta H}\rangle\mathbf{L}_1\langle e^{i\mathbf{p}_0\eta H}\rangle]^m\begin{cases}\mathbf{L}_2\overline{\mathbf{A}}_0^{-1}\tilde{\mathbf{u}}_0^{*(\infty)}(h_2) & \text{if } N \text{ is odd;}\\ \mathbf{L}_2\langle e^{-i\bar{\mathbf{p}}_0\eta H}\rangle\mathbf{L}_1\mathbf{A}_0^{-1}\tilde{\mathbf{u}}_0^{*(\infty)}(h_1) & \text{if } N \text{ is even,}\end{cases} \tag{B.12}$$

with

$$\mathbf{L}_1 = \overline{\mathbf{A}}_0^{-1}\left(\mathbf{M}_1-\overline{\mathbf{M}}_0\right)^{-1}(\mathbf{M}_0-\mathbf{M}_1)\mathbf{A}_0, \tag{B.13}$$

$$\mathbf{L}_2 = \mathbf{A}_0^{-1}\left(\overline{\mathbf{M}}_2-\mathbf{M}_0\right)^{-1}\left(\overline{\mathbf{M}}_0-\overline{\mathbf{M}}_2\right)\overline{\mathbf{A}}_0, \tag{B.14}$$

where $m = (N-1)/2$ if N is odd, and $(N-2)/2$ if N is even.

Appendix C. Direct 2D integral evaluation of trimaterial Green's functions

We mentioned previously that the physical-domain trimaterial Green's functions can also be evaluated directly using the 2D inverse Fourier transforms in the polar coordinate system, with sacrifice of intensive computational time. To check with our expansion solution, we give, in this appendix, a brief derivation for the direct 2D integral solution. We start with the general solutions in the Fourier-transformed domain described in Section 3. To derive the Green's functions in the trimaterials, one may first assign the homogeneous-domain solution with unknowns to each one of the media and solve for the unknowns by imposing the interfacial and radiation conditions, Eqs. (3)–(5). Explicitly, these homogeneous-domain solutions for each domain are given, in the Fourier-transformed domain, as a sum of an infinite-domain Green's function and a complementary part:

$$\tilde{\mathbf{u}}_0^*(y_1,y_2,x_3;\mathbf{X}) = e^{iy_\alpha X_\alpha}\left(\tilde{\mathbf{u}}_0^{*(\infty)}(y_1,y_2,x_3;X_3) + i\eta^{-1}\left[\overline{\mathbf{A}}_0\langle e^{-i\bar{\mathbf{p}}_0\eta(x_3-h_1)}\rangle\mathbf{V}_0 + \mathbf{A}_0\langle e^{-i\mathbf{p}_0\eta(x_3-h_2)}\rangle\mathbf{W}_0\right]\right), \tag{C.1}$$

$$\tilde{\mathbf{t}}_0^*(y_1,y_2,x_3;\mathbf{X}) = e^{iy_\alpha X_\alpha}\left(\tilde{\mathbf{t}}_0^{*(\infty)}(y_1,y_2,x_3;X_3) + \left[\overline{\mathbf{B}}_0\langle e^{-i\bar{\mathbf{p}}_0\eta(x_3-h_2)}\rangle\mathbf{V}_0 + \mathbf{B}_0\langle e^{-i\mathbf{p}_0\eta(x_3-h_1)}\rangle\mathbf{W}_0\right]\right), \tag{C.2}$$

$$\tilde{\mathbf{s}}_0^*(y_1,y_2,x_3;\mathbf{X}) = e^{iy_\alpha X_\alpha}\left(\tilde{\mathbf{s}}_0^{*(\infty)}(y_1,y_2,x_3;X_3) + \left[\overline{\mathbf{C}}_0\langle e^{-i\bar{\mathbf{p}}_0\eta(x_3-h_2)}\rangle\mathbf{V}_0 + \mathbf{C}_0\langle e^{-i\mathbf{p}_0\eta(x_3-h_1)}\rangle\mathbf{W}_0\right]\right), \tag{C.3}$$

for $h_1 < x_3 < h_2$ (material 0),

$$\tilde{\mathbf{u}}_1^*(y_1,y_2,x_3;\mathbf{X}) = e^{iy_\alpha X_\alpha}\left(\tilde{\mathbf{u}}_1^{*(\infty)}(y_1,y_2,x_3;X_3) + i\eta^{-1}\mathbf{A}_1\langle e^{-i\mathbf{p}_1\eta(x_3-h_1)}\rangle\mathbf{W}_1\right), \tag{C.4}$$

$$\tilde{\mathbf{t}}_1^*(y_1,y_2,x_3;\mathbf{X}) = e^{iy_\alpha X_\alpha}\left(\tilde{\mathbf{t}}_1^{*(\infty)}(y_1,y_2,x_3;X_3) + \mathbf{B}_1\langle e^{-i\mathbf{p}_1\eta(x_3-h_1)}\rangle\mathbf{W}_1\right), \tag{C.5}$$

$$\tilde{\mathbf{s}}_1^*(y_1,y_2,x_3;\mathbf{X}) = \mathrm{e}^{\mathrm{i}y_\alpha X_\alpha}\left(\tilde{\mathbf{s}}_1^{*(\infty)}(y_1,y_2,x_3;X_3) + \mathbf{C}_1\langle \mathrm{e}^{-\mathrm{i}\bar{\mathbf{p}}_1\eta(x_3-h_1)}\rangle \mathbf{W}_1\right), \tag{C.6}$$

for $x_3 < h_1$ (material 1), and

$$\tilde{\mathbf{u}}_2^*(y_1,y_2,x_3;\mathbf{X}) = \mathrm{e}^{\mathrm{i}y_\alpha X_\alpha}\left(\tilde{\mathbf{u}}_2^{*(\infty)}(y_1,y_2,x_3;X_3) + \mathrm{i}\eta^{-1}\overline{\mathbf{A}}_2\langle \mathrm{e}^{-\mathrm{i}\bar{\mathbf{p}}_2\eta(x_3-h_2)}\rangle \mathbf{V}_2\right), \tag{C.7}$$

$$\tilde{\mathbf{t}}_2^*(y_1,y_2,x_3;\mathbf{X}) = \mathrm{e}^{\mathrm{i}y_\alpha X_\alpha}\left(\tilde{\mathbf{t}}_2^{*(\infty)}(y_1,y_2,x_3;X_3) + \overline{\mathbf{B}}_2\langle \mathrm{e}^{-\mathrm{i}\bar{\mathbf{p}}_2\eta(x_3-h_2)}\rangle \mathbf{V}_2\right), \tag{C.8}$$

$$\tilde{\mathbf{s}}_2^*(y_1,y_2,x_3;\mathbf{X}) = \mathrm{e}^{\mathrm{i}y_\alpha X_\alpha}\left(\tilde{\mathbf{s}}_2^{*(\infty)}(y_1,y_2,x_3;X_3) + \overline{\mathbf{C}}_2\langle \mathrm{e}^{-\mathrm{i}\bar{\mathbf{p}}_2\eta(x_3-h_2)}\rangle \mathbf{V}_2\right), \tag{C.9}$$

for $x_3 > h_2$ (material 2). Note that for $x_3 < h_1$ and $x_3 > h_2$, the radiation condition, Eq. (5) has been satisfied, retaining one of the tensors **V** and **W** as unknown.

Substituting the above expressions into Eqs. (3) and (4) results in four independent equations, with four unknown tensors $\mathbf{V}_0$, $\mathbf{W}_0$, $\mathbf{V}_1$ and $\mathbf{W}_2$, for given y_1 and y_2, and a fixed X_3, as

$$\tilde{\mathbf{u}}_1^{*(\infty)}(h_1) - \tilde{\mathbf{u}}_0^{*(\infty)}(h_1) = \mathrm{i}\eta^{-1}\left(\overline{\mathbf{A}}_0\mathbf{V}_0 + \mathbf{A}_0\langle \mathrm{e}^{\mathrm{i}\mathbf{p}_0\eta H}\rangle \mathbf{W}_0 - \mathbf{A}_1\mathbf{W}_1\right), \tag{C.10}$$

$$\tilde{\mathbf{t}}_1^{*(\infty)}(h_1) - \tilde{\mathbf{t}}_0^{*(\infty)}(h_1) = \overline{\mathbf{B}}_0\mathbf{V}_0 + \mathbf{B}_0\langle \mathrm{e}^{\mathrm{i}\mathbf{p}_0\eta H}\rangle \mathbf{W}_0 - \mathbf{B}_1\mathbf{W}_1, \tag{C.11}$$

$$\tilde{\mathbf{u}}_2^{*(\infty)}(h_2) - \tilde{\mathbf{u}}_0^{*(\infty)}(h_2) = \mathrm{i}\eta^{-1}\left(\overline{\mathbf{A}}_0\langle \mathrm{e}^{-\mathrm{i}\bar{\mathbf{p}}_0\eta H}\rangle \mathbf{V}_0 + \mathbf{A}_0\mathbf{W}_0 - \overline{\mathbf{A}}_2\mathbf{V}_2\right), \tag{C.12}$$

$$\tilde{\mathbf{t}}_2^{*(\infty)}(h_2) - \tilde{\mathbf{t}}_0^{*(\infty)}(h_2) = \overline{\mathbf{B}}_0\langle \mathrm{e}^{-\mathrm{i}\bar{\mathbf{p}}_0\eta H}\rangle \mathbf{V}_0 + \mathbf{B}_0\mathbf{W}_0 - \overline{\mathbf{B}}_2\mathbf{V}_2, \tag{C.13}$$

where the arguments y_1 and y_2 and X_3 in the functions are omitted for simplicity and will be resumed as necessary for clarity. Solving this set of equations gives $\mathbf{V}_0$ in the form,

$$\mathbf{V}_0 = (\mathbf{E}-\mathbf{F})^{-1}\left[\left(\mathbf{A}_1^{-1}\mathbf{A}_0 - \mathbf{B}_1^{-1}\mathbf{B}_0\right)^{-1}\mathbf{D}_{01} - \langle \mathrm{e}^{\mathrm{i}\mathbf{p}_0\eta H}\rangle\left(\overline{\mathbf{A}}_2^{-1}\mathbf{A}_0 - \overline{\mathbf{B}}_2^{-1}\mathbf{B}_0\right)^{-1}\mathbf{D}_{02}\right], \tag{C.14}$$

with

$$\mathbf{D}_{01} = -\mathrm{i}\eta\mathbf{A}_1^{-1}\left(\tilde{\mathbf{u}}_1^{*(\infty)}(h_1) - \tilde{\mathbf{u}}_0^{*(\infty)}(h_1)\right) - \mathbf{B}_1^{-1}\left(\tilde{\mathbf{t}}_1^{*(\infty)}(h_1) - \tilde{\mathbf{t}}_0^{*(\infty)}(h_1)\right), \tag{C.15}$$

$$\mathbf{D}_{02} = -\mathrm{i}\eta\overline{\mathbf{A}}_2^{-1}\left(\tilde{\mathbf{u}}_2^{*(\infty)}(h_2) - \tilde{\mathbf{u}}_0^{*(\infty)}(h_2)\right) - \overline{\mathbf{B}}_2^{-1}\left(\tilde{\mathbf{t}}_2^{*(\infty)}(h_2) - \tilde{\mathbf{t}}_0^{*(\infty)}(h_2)\right), \tag{C.16}$$

$$\mathbf{E} = \left(\mathbf{A}_1^{-1}\mathbf{A}_0 - \mathbf{B}_1^{-1}\mathbf{B}_0\right)^{-1}\left(\mathbf{A}_1^{-1}\overline{\mathbf{A}}_0 - \mathbf{B}_1^{-1}\overline{\mathbf{B}}_0\right), \tag{C.17}$$

$$\mathbf{F} = \langle \mathrm{e}^{\mathrm{i}\mathbf{p}_0\eta H}\rangle\left(\overline{\mathbf{A}}_2^{-1}\mathbf{A}_0 - \overline{\mathbf{B}}_2^{-1}\mathbf{B}_0\right)^{-1}\left(\overline{\mathbf{A}}_2^{-1}\overline{\mathbf{A}}_0 - \overline{\mathbf{B}}_2^{-1}\overline{\mathbf{B}}_0\right)\langle \mathrm{e}^{-\mathrm{i}\bar{\mathbf{p}}_0\eta H}\rangle. \tag{C.18}$$

Consequently, other three unknown tensors can be derived sequentially, as

$$\mathbf{W}_0 = \left(\overline{\mathbf{A}}_2^{-1}\mathbf{A}_0 - \overline{\mathbf{B}}_2^{-1}\mathbf{B}_0\right)^{-1}\left[\mathbf{D}_{02} - \left(\bar{\mathbf{A}}_2^{-1}\bar{\mathbf{A}}_0 - \overline{\mathbf{B}}_2^{-1}\bar{\mathbf{B}}_0\right)\langle \mathrm{e}^{-\mathrm{i}\bar{\mathbf{p}}_0\eta H}\rangle \mathbf{V}_0\right], \tag{C.19}$$

$$\mathbf{W}_1 = \mathbf{A}_1^{-1}\left[\overline{\mathbf{A}}_0\mathbf{V}_0 + \mathbf{A}_0\langle \mathrm{e}^{\mathrm{i}\mathbf{p}_0\eta H}\rangle \mathbf{W}_0 + \mathrm{i}\eta\left(\tilde{\mathbf{u}}_1^{*(\infty)}(h_1) - \tilde{\mathbf{u}}_0^{*(\infty)}(h_1)\right)\right], \tag{C.20}$$

$$\mathbf{V}_2 = \overline{\mathbf{A}}_2^{-1}\left[\overline{\mathbf{A}}_0\langle \mathrm{e}^{-\mathrm{i}\bar{\mathbf{p}}_0\eta H}\rangle \mathbf{V}_0 + \mathbf{A}_0\mathbf{W}_0 + \mathrm{i}\eta\left(\tilde{\mathbf{u}}_2^{*(\infty)}(h_2) - \tilde{\mathbf{u}}_0^{*(\infty)}(h_2)\right)\right]. \tag{C.21}$$

Finally, by substituting these tensors back into the expressions for $\tilde{\mathbf{u}}^*$, $\tilde{\mathbf{t}}^*$ and $\tilde{\mathbf{s}}^*$ in Eqs. (C.1)–(C.9), a solution to the trimaterial Green's functions in the transformed domain is obtained as a sum of the infinite-space Green's solution and a complementary term. Simply by substituting the transformed-domain solution into the inverse-transform operator, Eq. (20) or (21), the corresponding physical-domain solution is obtained in terms of a 2D integral over an infinite plane. This integral is carried out by an adaptive quadrature scheme. We emphasize, however, the 2D integral is only needed for the complementary part of the Fourier-domain solution since the infinite-space Green's function is already available in an explicit form (Ting and Lee, 1997; Tonon et al., 2001). Such a partition of the trimaterial solution into an infinite-space solution and a complementary part has the advantage of avoiding numerical integral of singular function as the singularity is involved in the infinite-space solution only (Pan and Yuan, 2000).

References

Barnett, D.M., Lothe, J., 1975. Line force loadings on anisotropic half-spaces and wedges. Physica Norvegica 8, 13–22.

Chiu, Y.T., Wu, K.C., 1998. Analysis for elastic strips under concentrated loads. ASME Journal of Applied Mechanics 65, 626–634.

Chou, Y.T., 1966. Screw dislocations in and near lamellar inclusions. Physical Status of Solids 17, 509–516.

Fares, N., Li, V.C., 1988. General image method in a plane-layered elastostatic medium. ASME Journal of Applied Mechanics 55, 781–785.

Freund, L.B., 1994. The mechanics of dislocations in strained-layer semiconductor materials. Advances in Applied Mechanics 30, 1–66.

Gao, H., Nix, W.D., 1999. Surface roughening of heteroepitaxial thin films. Annual Review of Materials Science 29, 173–209.

Hsueh, C.H., 2000. Analysis of edge effects on residual stresses in film strip/substrate systems. Journal of Applied Physics 88, 3022–3028.

Hu, S.M., 1991. Stress-related problems in silicon technology. Journal of Applied Physics 70, R53–R80.

Hutchinson, J.W., Suo, Z., 1991. Mixed mode cracking in layered materials. Advances in Applied Mechanics 29, 63–191.

Jenichen, B., Kaganer, V.M., Riedel, A., Kostial, H., Gong, Q., Hey, R., Friedland, K., 2001. Deformations in (Al,Ga)As epitaxial layers wafer bonded on dissimilar substrates. Journal of Applied Physics 89, 2173–2178.

Jones, R.M., 1999. Mechanics of Composite Materials, second ed. Taylor & Francis, Inc, Philadelphia, PA, USA.

Liu, X.H., Suo, Z., Ma, Q., Fujimoto, H., 2000. Developing design rules to avert cracking and debonding in integrated circuit structures. Engineering Fracture Mechanics 66, 387–402.

Matemilola, S.A., Stronge, W.J., 1995. Diffusion rate for stress in orthotropic materials. ASME Journal of Applied Mechanics 62, 654–661.

Mindlin, R.D., 1936. Force at a point in the interior of a semi-infinite solid. Physics 7, 195–202.

Pagano, N.J., 1978a. Stress fields in composite laminates. International Journal of Solids and Structures 14, 385–400.

Pagano, N.J., 1978b. Free edge stress fields in composite laminates. International Journal of Solids and Structures 14, 401–406.

Pan, E., 1997. Static Green's functions in multilayered half spaces. Applied Mathematical Modelling 21, 509–521.

Pan, E., Yang, B., 2001. Elastostatic fields in an anisotropic substrate due to a buried quantum dot. Journal of Applied Physics 90, 6190–6196.

Pan, E., Yang, B., 2002. Three-dimensional interfacial Green's functions in anisotropic bimaterials. Applied Math. Modelling, under review.

Pan, E., Yuan, F.G., 2000. Three-dimensional Green's functions in anisotropic bimaterials. International Journal of Solids and Structures 37, 5329–5351.

Pan, E., Yang, B., Cai, G., Yuan, F.G., 2001. Stress analyses around holes in composite laminates using boundary element method. Engineering Analysis with Boundary Elements 25, 31–40.

Pearson, G.S., Faux, D.A., 2000. Analytical solutions for strain in pyramidal quantum dots. Journal of Applied Physics 88, 730–736.

Schoeppner, G.A., Pagano, N.J., 1998. Stress fields and energy release rates in cross-ply laminates. International Journal of Solids and Structures 35, 1025–1055.

Schweitz, K.O., Bottiger, J., Chevallier, J., Feidenhansl, R., Nielsen, M.M., Rasmussen, F.B., 2000. Interface stress in Au/Ni multilayers. Journal of Applied Physics 88, 1401–1406.

Shou, K.J., 2000. A superposition scheme to obtain fundamental boundary element solutions in multi-layered elastic media. International Journal for Numerical and Analytical Methods in Geomechanics 24, 795–814.

Shou, K.J., Napier, J.A.L., 1999. A two-dimensional linear variation displacements discontinuity method for three-layered elastic media. International Journal of Rock Mechanics and Mining Sciences 36, 719–729.

Suhir, E., 2000. Predicted thermally induced stresses in, and the bow of, a circular substrate/thin-film structure. Journal of Applied Physics 88, 2363–2370.

Suhir, E., 2001. Predicted thermal stresses in a bimaterial assembly adhesively bonded at the ends. Journal of Applied Physics 89, 120–129.

Suo, Z., Hutchinson, J.W., 1989. Steady-state cracking in brittle substrates beneath adherent films. International Journal of Solids and Structures 25, 1337–1353.

Ting, T.C.T., 1996. Anisotropic Elasticity. Oxford University Press, Oxford.

Ting, T.C.T., Lee, V.G., 1997. The three-dimensional elastostatic Green's function for general anisotropic linear elastic solids. Quarterly Journal of Mechanics and Applied Mathematics 50, 407–426.

Tonon, F., Pan, E., Amadei, B., 2001. Green's functions and boundary element formulation for 3D anisotropic media. Computers and Structures 79, 469–482.

Yu, H.Y., Sanday, S.C., 1993. Elastic fields due to centers of dilatation and thermal inhomogeneities in plane-layered solids. Journal of the Mechanics and Physics in Solids 41, 267–296.

Wu, K.C., 1998. Generalization of the Stroh formalism to 3-dimensional anisotropic elasticity. Journal of Elasticity 51, 213–225.